Review Article

Hamid Mahmoudi, Maedeh Mahmoudi, Omid Doustdar, Hessam Jahangiri, Athanasios Tsolakis, Sai Gu, and Miroslaw Lech Wyszynski*

A review of Fischer Tropsch synthesis process, mechanism, surface chemistry and catalyst formulation

https://doi.org/10.1515/bfuel-2017-0002
Received Mar 09, 2017; accepted Nov 20, 2017

Abstract: For more than half a century, Fischer-Tropsch synthesis (FTS) of liquid hydrocarbons was a technology of great potential for the indirect liquefaction of solid or gaseous carbon-based energy sources (Coal-To-Liquid (CTL) and Gas-To-Liquid (GTL)) into liquid transportable fuels. In contrast with the past, nowadays transport fuels are mainly produced from crude oil and there is not considerable diversity in their variety. Due to some limitations in the first generation bio-fuels, the Second-Generation Biofuels (SGB)' technology was developed to perform the Biomass-To-Liquid (BTL) process. The BTL is a well-known multi-step process to convert the carbonaceous feedstock (biomass) into liquid fuels via FTS technology. This paper presents a brief history of FTS technology used to convert coal into liquid hydrocarbons; the significance of bio-energy and SGB are discussed as well. The paper covers the characteristics of biomass, which is used as feedstock in the BTL process. Different mechanisms in the FTS process to describe carbon monoxide hydrogenation as well as surface polymerization reaction are discussed widely in this paper. The discussed mechanisms consist of carbide, CO-insertion and the hydroxycarbene mechanism. The surface chemistry of silica support is discussed. Silanol functional groups in silicon chemistry are explained extensively. The catalyst formulation in the Fischer Tropsch (F-T) process as well as F-T reaction engineering is discussed. In addition, the most common catalysts are introduced and the current reactor technologies in the F-T indirect liquefaction process are considered.

Keywords: Fischer Tropsch, Silica, Cobalt catalyst, fixed bed reactor, bio-fuel and biomass

***Corresponding Author: Miroslaw Lech Wyszynski:** Department of Mechanical Engineering, School of Engineering, College of Engineering and Physical Sciences, The University of Birmingham, Birmingham, B15 2TT, United Kingdom; Email: m.l.wyszynski@bham.ac.uk; Tel.: +44 121 414 4159

1 Fischer-Tropsch Synthesis (FTS) process overview

1.1 Introduction

The over-reliance of the world's nations on conventional fossil fuels puts our planet in peril. The continuity of the current situation will result in the rise of a combined average temperature over global land and ocean surfaces by 5°C in 2100, bringing a rise in sea levels, food and water shortages and an increase in extreme weather events. The global warming, caused by humans, is one of the biggest threats to our future well-being [1]. In addition, oil reserves are limited and these reserves are decreasing dramatically. This reduction alongside the other relevant economic factors affects the world's oil prices. The need to run engines with the new generation of liquid fuels is inevitable. The investigations by the US Energy Information Administration (EIA) published in 2013 expressed a 56 percent increase in the world's energy consumption by the year 2040. Total world energy demand will have risen to 865 EJ (exajoule) by this year. The total world energy consumption was reported as 553 EJ in 2010. The outlook indicates that renewable energy is one of the fastest-growing energy sources in the world; where its usage increases 2.5 percent per year. Despite increasing success in the renewable energies, it is predicted that the fossil fuels will supply al-

Hamid Mahmoudi, Maedeh Mahmoudi, Omid Doustdar, Athanasios Tsolakis: Department of Mechanical Engineering, School of Engineering, College of Engineering and Physical Sciences, The University of Birmingham, Birmingham, B15 2TT, United Kingdom
Hessam Jahangiri: Cranfield University, White Building, Cranfield, Bedfordshire, MK43 0AL, United Kingdom; European Bioenergy Research Institute (EBRI), Aston University, The Aston Triangle, Birmingham, B4 7ET, United Kingdom
Sai Gu: Department of Chemical and Process Engineering, Faculty of Engineering and Physical Sciences, University of Surrey, Guilford, GU2 7XH, United Kingdom

Open Access. © 2017 H. Mahmoudi *et al.*, published by De Gruyter Open. BY-NC-ND This work is licensed under the Creative Commons Attribution-NonCommercial-NoDerivatives 4.0 License

most 80 percent of the world's energy demand through to 2040 [2, 3].

1.2 History of F-T Synthesis

Fischer-Tropsch synthesis (FTS) has drawn a great deal of interest in the recent decades from researchers, since it has been believed that liquid hydrocarbons' production through this promising clean technology is a potential alternative method which could solve the shortage of liquid transport fuels [4–6]. Second generation bio-fuels can be made from cellulosic biomass by thermal production of syngas followed by Fischer-Tropsch synthesis. This process is known as the Biomass-To-Liquid (BTL) process for producing liquid fuels [6, 7]. F-T synthesis is a technology that has an extensive history of production of gasoline and diesel from coal and natural gas. Recently great interest has been generated in applying this relatively well-known technology to cellulosic biomass and agricultural waste, to convert them to linear- and branched-chain synthetic hydrocarbon (HCs).

The Bergius coal liquefaction and Fischer-Tropsch synthesis of liquid hydrocarbons were invented and subsequently developed between the years 1910 to 1926. The first step to overcome the lack of petroleum by synthesising Germany's abundant coal supplies was taken by Friedrich Bergius (1884-1949) (shown in Figure 1), who invented high-pressure coal hydrogenation in Rheinau-Mannheim during the first and second decades of the 20th century. Bergius prepared a coal-oil paste by crushing and dissolving the coals containing less than 85 percent carbon in heavy oil; afterwards he reacted the prepared paste with hydrogen gas at 200 atm and 673 K; the resulting products were petroleum-like liquids [8].

In 1926, a decade after this success by German scientists, Franz Fischer and Hans Tropsch (shown in Figure 1) invented a process to convert coal into synthetic liquid hydrocarbons at the Kaiser Wilhelm Institute for Coal Research (KWI) in Mulheim Ruhr. First, Fischer and Tropsch hydrocracked the coal by reacting it with steam to produce synthesis gas (mixture of carbon monoxide and hydrogen) and then converted the gases to petroleum-like synthetic liquid at 1 to 10 atm and 453 to 473 K. The cobalt catalyst was first designed and developed by Fischer and his coworker, Tropsch to achieve a successful process [8].

Among the industrialized nations, Germany was the first to synthesize petroleum from coal.

From the early 1930s to the end of the 20th century, Germany exported the technologically successful F-T plant to the United States of America, Britain, Japan, France, South Africa and other nations. In Britain, the University of Birmingham was the pioneer in performing laboratory scale and pilot-plant sized Fischer-Tropsch synthesis investigations in 1920 [8]. Thenceforward, Germany and Britain were the most successful and pioneering in developing the generation of liquid synthetic hydrocarbons through F-T technology. The serious practical work on F-T synthesis in the US was began post-World War II; after that a rapid increase in petroleum consumption was observed leading to considerable concern from government [8].

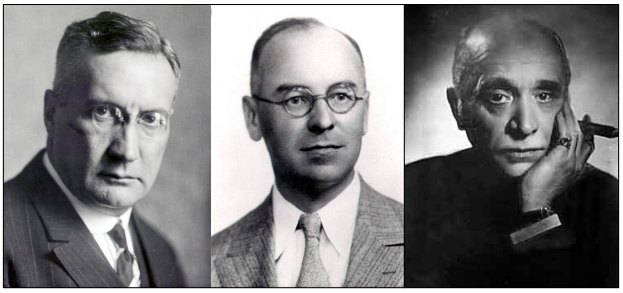

Figure 1: Franz Fischer (left) and Hans Tropsch (middle), inventors of Fischer-Tropsch Synthesis (FTS) process and Friedrich Bergius (right) coal liquefaction process inventor [8, 9]

1.3 Significance of bio-energy

Renewable energies such as bio diesel will play a significant role in the future for transporting energies, due to the abundant advantages of this fuel. Production of bio diesel from biomass decreases the cost of the required fuel for farmers in comparison to oil/liquefied petroleum gas (LPG), because this fuel is produced by the farmer and there is no transporting cost and moreover, the feedstock is much cheaper than fossil fuels. In addition, bio-fuels are produced from plant waste that can be re-planted and re-grown by the interaction of carbon dioxide, water, air, soil and sunlight, which guarantees the future transportation energies' sustainability. Biodiesel made from biomass could easily replace fossil fuels due to its compatibility with the current engines' technology and their existing fuel system. Running the engines with biodiesel produced from vegetable oils such as canola or rapeseeds, which are low in saturated fat, could prevent the formation of ice in frigid temperatures and subsequently prevent the vehicle's engine struggling with ice crystals. Production of bio fuels via sustainable energy crops could not solve the country's energy problem, but could reduce the dependency on foreign oil. The bitter experience of the industrialized countries in 1973, caused by the oil-producing countries of the Middle East, whereby they stopped exporting

oil, propelled the western countries to become independent of them for their oil supplies [10].

Biodiesel refineries are much cleaner than those of crude oil during the conversion of biomass into usable liquid products. The conventional fuel refineries release millions of pounds (lbs) of cancer-causing chemicals such as benzene (C_6H_6), butadiene (C_4H_6) and formaldehyde (CH_2O) into the environment as well as nickel, sulphur dioxide (SO_2), lead and some other pollutants which cause heart disease and asthma. It is therefore the case that bio-fuel refineries are much more environmentally friendly [10].

Biodiesel produced via the Fischer-Tropsch synthesis (FTS) process seems to be a highly-promising alternative fuel due to such attractive specifications. Ultra-clean fuel, high cetane number of final liquid products, virtually zero emissions of sulphur compounds and aromatic hydrocarbons are some of the significant advantages of bio-fuel derived from F-T clean technology [11, 12]. Utilization of biodiesel with compatible engines not only lowers the emissions of engines running on this fuel (nitrogen oxide (NO_x), particulate matter (PM) and greenhouse gases (GHG)) also improve the catalytic after-treatment process [13]. The low emission of carbon monoxide, nitrogen monoxide, hydrocarbons and low sulphur and aromatic compounds make the synthetic fuels green and liquid clean fuels [14]. The absence of these compounds and the high cetane number of the generated products lead to high performance biodiesel through F-T technology. The measurements of exhaust particle number concentration and size distribution in an engine fuelled with Gas-To-Liquid (GTL) are lower than those of an engine fuelled with conventional diesel [15].

The investigation of Public Health England (PHE) revealed that 5.3 percent of all the deaths in people aged over 25 correspond to air pollution. Under the Climate Change Act 2008, the UK Government is legally required to reduce the emission of GHG by 80% by the year 2050 [16]. The application of ultra-clean biodiesel by the farmers not only helps to reduce the emission of GHG but also lowers the emission of cancer-causing pollutants. This is one of the successful deliverables in the exploitation of renewable energies which benefits public health. The UK's Renewable Transport Fuels Obligation (RTFO) required the suppliers of fossil fuels to target 2.6% of road fuels to be made up of renewable fuels in 2011. This obligation first came into effect in 2008 and in that year, 84% from 1 million tonnes of bio-fuels in the UK market was made up of biodiesel. The primary pathway of previous investigations in achieving an industrial impact is the significant advantage of a fixed-bed reactor which could be easily scaled up for commercial plant. The success in commercialisation of bio-fuel generators could be effective in contributing to the achievement of a 13 percent substitution of bio-energy by volume in 2020 [17]. The exploitation of the bio-fuel generator in the agricultural industry could decrease the fuel demand by this sector. In addition, according to the report of the Biotechnology Industry Organization, the bio technology industry is expected to create 190,000 direct "green jobs" in the US. The commercialisation of bio-fuel generators in the UK will benefit society directly by creating new green job opportunities in United Kingdom [18].

2 Characteristics of biomass

In general, biomass is ascribed to the non-fossilized and biodegradable organic materials that have been derived from plants, animals and micro-organisms. The products of decomposition of non-fossilized organic materials are also referred to as biomass. The botanical (plant species) or biological (animal wastes and carcass) sources of biomass could be classified into agricultural, forest, municipal, energy and biological sources. The process of conversion of carbon dioxide into the botanical biomass (carbohydrate) in the presence of chlorophyll II and water is represented in reaction 1. Green plants break down the water in the presence of a particular wavelength of solar energy to obtain electrons and protons so that the carbon dioxide is converted into glucose (CH_mO_n).

$$\begin{pmatrix}\text{living}\\ \text{plant}\end{pmatrix} + CO_2 + H_2O + \text{sunlight} \xrightarrow{\text{Chlorophyll}} (CH_mO_n) + O_2 - 480\ \left(\frac{\text{kJ}}{\text{mol}}\right) \quad (1)$$

As represented in the above equation, for each mole of carbon dioxide absorbed, 1 mole of oxygen is released. Cellulose, hemicellulos and lignin are the three major constituents of non-starch and fibrous ligno-cellulose biomass. This kind of biomass is not part of the human food chain as it is not easily digestible by humans. There is a great interest in the cultivation of ligno-cellulosic plants (willow, switch grass etc.) that are grown fast and yield a high amount of energy per unit of land. Unlike lignocellulose, carbohydrates are dissolved easily and could be converted into liquid fuels quickly. This is the reason that most of the commercial ethanol plants utilize crops [19].

The polymeric constituents of biomass widely vary in different biomasses. Cellulose is the most common organic compound on the earth which forms the cell walls of biomass' structural components. Cellulose ($(C_6H_{10}O_5)_n$) is

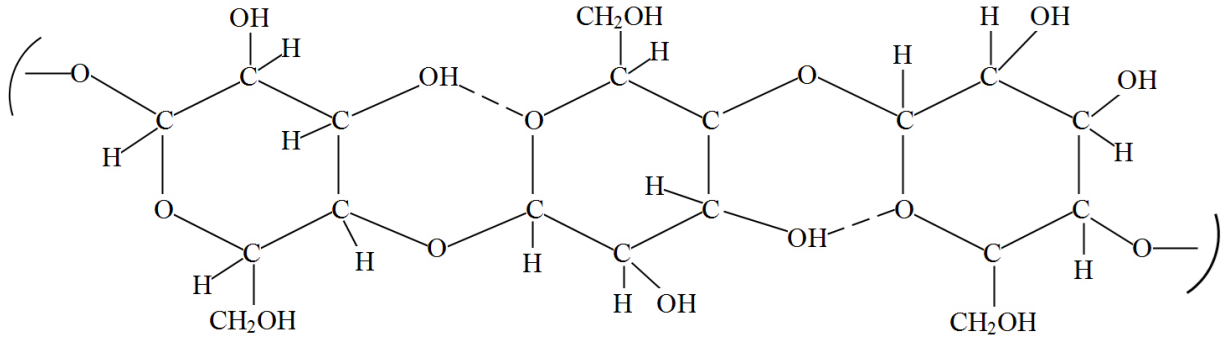

Figure 2: Molecular structure of biomass' cellulose constituent [19]

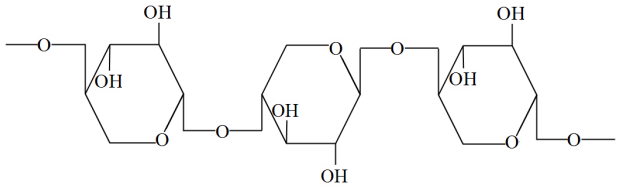

Figure 3: Hemicellulose (xylan) molecular structure [19]

a long chain polymer with a crystalline structure which is made up of many molecules of glucose. Figure 2 indicates the molecular structure of cellulose. Cellulose is made up of about 40 – 44 percent of dry wood weight which is not digestible by humans [19].

Hemicellulose is an amorphous branched chain hydrocarbon structure of a cell wall's constituent (shown in Figure 3). While cellulose has a high degree of polymerization (~10,000), hemicellulose has a lower degree of polymerization (~100-200). The generic formula of hemicellulose is represented as $(C_5H_8O_4)_n$.; unlike cellulose resistant to hydrolysis, hemicellulose is hydrolyzed easily and solved in a solution of weak alkaline. Twenty to thirty percent of dry weight wood is made by hemicellulose. The hemicellulosic constituent of biomass cells yields less tar and more gases than the cellulosic constituent [19].

About 18 to 25 percent of a typical hardwood is made of a highly insoluble lignin constituent with a highly branched polymer of phenyl propane as shown in Figure 4. These plentiful organic polymers in the earth make up the secondary cell walls of plants. Lignins act as cementing agents which hold the adjacent cells together [19].

The higher hydrogen-to-carbon (H:C) ratio as well as high oxygen-to-carbon (O:C) ratio in fresh biomass, such as leaves, are correlated to the lower efficacious heating value of these plants. A high amount of oxygen contents in biomass is not useful for the heating value of hydrocarbon fuel and makes the biomass liquefaction process more difficult. Moreover, the H:C ratio of biomass as well as its O:C ratio is much higher than that of fossil fuel. Equation (2) represents the linear function of these two ratios in a wide range of biomass:

$$(H : C) = 1.4125\,(O : C) + 0.5004 \quad (2)$$

The heating value of the biomass is related to its geological age meaning that the atomic ratio is increased in older fuels. Higher energy content results from biomass with a higher atomic ratio which increases with the increasing of the biomass' age. Moreover, the biomass with the same cellulose to lignin ratio and hemicellulose to lignin ratio, irrespective of their type, show similar behaviour in the transformation process [19].

Municipal solid waste (MSW) is an important source of secondary waste that is derived from renewable (food scraps, paper etc) and non-renewable primary biomass (plastic, glass and metals). Refuse-derived fuel (RDF) is combustible part of MSW secondary waste. Sewage sludge is considered as an important biomass source. Aerobic and anaerobic digestions are two types of degradation process to reduce the amount of biodegradable waste. CO_2, H_2O and air are the products or microorganism's degradation process in aerobic digestion; while the second process produces methane. In anaerobic digestion, the leachate is collected from the landfill and pumped back in the absence of oxygen and the presence of methanogenic bacteria (thermophile, mesophile and psychophile) to the sealed land-filled solids. Equation (3) represents the exothermic biodegradation reaction which produces water and carbon dioxide. Methane is known as 21 times stronger than carbon dioxide among the greenhouse gases.

$$C_6H_{12}O_6(\text{representing waste}) + \text{bacteria} \rightarrow 3CO_2 + 3CH_4 + \text{digestate} \quad (3)$$

The United Kingdom Department of Energy and Climate Change estimated the availability of biomass as 6.1 to 15.3 Million Oven Dried Tonnes (MODT) in the year 2011;

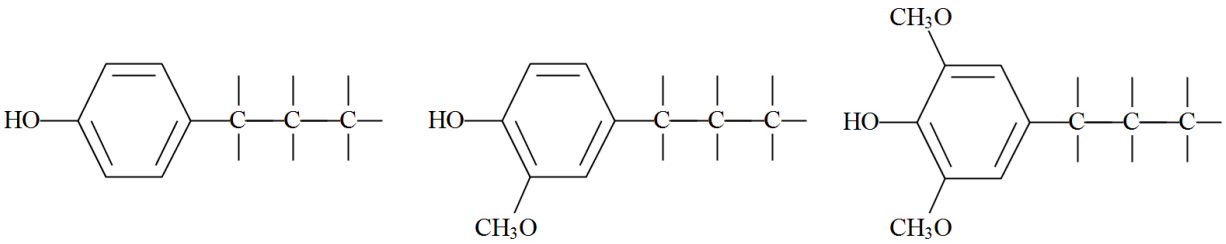

Figure 4: Structural units of lignin, 4-propenyl phenol (left), 4-propenyl-2-methoxy phenol (middle) and 4-propenyl-2.5-dimethoxyl phenol (right) [9, 19]

8.1 to 15.5 MODT in 2015 and 10.4 to 16.3 MODT in 2020. Of these amounts, 3.2 to 5.0 MODT are estimated amounts of dry agricultural residue in 2015, with 3.7 to 5.0 MODT in 2020. On top of this, between 3.2 and 4.3 MODT are estimated amounts of waste wood which are expected in the years 2015 and 2020 respectively [20].

3 Fischer-Tropsch Synthesis mechanisms

Fischer-Tropsch synthesis is a surface polymerization reaction in which the reaction between the reagents, hydrogen and carbon monoxide, takes place on the surface of the catalyst in situ. First, reagents form monomer units. These building blocks are subsequently polymerized to yield a wide spectrum of the products (mainly paraffin) ranging from C_1 to C_{40} HCs (heavy wax products) [21]. Several simultaneous chemical reactions occur in the F-T regime producing desired and undesired products. Reactions (4) to (7) summarize the general forms of the reactions that take place in Fischer-Tropsch synthesis of hydrocarbons (paraffins, olefins and alcohols); whereby the term -CH_2- represents a methylene group of normal paraffin. Polymerization of these blocks yields the products which depend on the thermodynamics and kinetics of the reactions [22]. Alkanes are the most preferred products in the F-T process. The produced alkanes from Equation (4) are mainly straight-chain hydrocarbons; while the alkene outputs of Equation (5) are mostly tertiary [23]. Equations (6) and (7) represent the general reaction forms which lead to formation of oxygenated products.

$$\text{Alkanes}: \quad nCO + (2n+1)\,H_2 \rightarrow H(CH_2)_{nH} + nH_2O \tag{4}$$

$$\text{Alkenes}: \quad nCO + 2nH_2 \rightarrow (CH_2)_n + nH_2O \tag{5}$$

$$\text{Alcohol}: \quad nCO + 2nH_2 \rightarrow H(CH_2)_{nOH} + (n-1)H_2O \tag{6}$$

$$\text{Carbonyls}: \quad nCO + (2n-1)H_2 \rightarrow (CH_2)_nO + (n-1)H_2O \tag{7}$$

The portion of each of the above hydrocarbons in synthetic crude oil corresponds to the synthesis conditions and the catalytic bed in which the synthesis is conducted. Regardless of the reactions parameters, all of the F-T reactions mechanisms are based on the ability of the metallic elements of the catalyst to dissociative chemisorb the carbon monoxide.

The mechanisms of the Fischer-Tropsch synthesis process have attracted many researchers in the past; such as B. H. Davis [24] and A. P. Anderson [25]. The definition of the complex reaction networks could describe the formation of carbon-carbon bonds, the hydrogenation of the carbon monoxide, as well as how subsequently the Fischer-Tropsch synthesis proceeds. These investigations lead to a comprehension of the F-T catalytic chemical surface reaction which could improve the design of F-T catalysts in the future. Different mechanisms based on different intermediates were proposed to govern the F-T syncrude composition. Carbide mechanism, CO insertion and hydroxycarbene mechanism are the main polymerization schemes that have been proposed within the three major steps (initiation, propagation and chain termination steps). The mechanisms differ with the nature of the formation of monomer units and the paths that the surface reactions govern which are to be converted to the proposed hydrocarbons.

In a carbide mechanism, adsorption of carbon monoxide on the catalyst surface initiates the F-T reaction. The initiation step results in the metal surface (M) being carbided by gaseous carbon monoxide. Carbon monoxide is chemisorbed initially in a bridge mode involving two surface sites of the catalyst and also is equilibrated in with a linear mode involving only one site of the metal surface. The C-O bond is subsequently dissociated into the C and O surface species. Hydrogen as the second reactant is chemisorbed and dissociated on the metal surface site as well [23]. While it is the case that carbon monox-

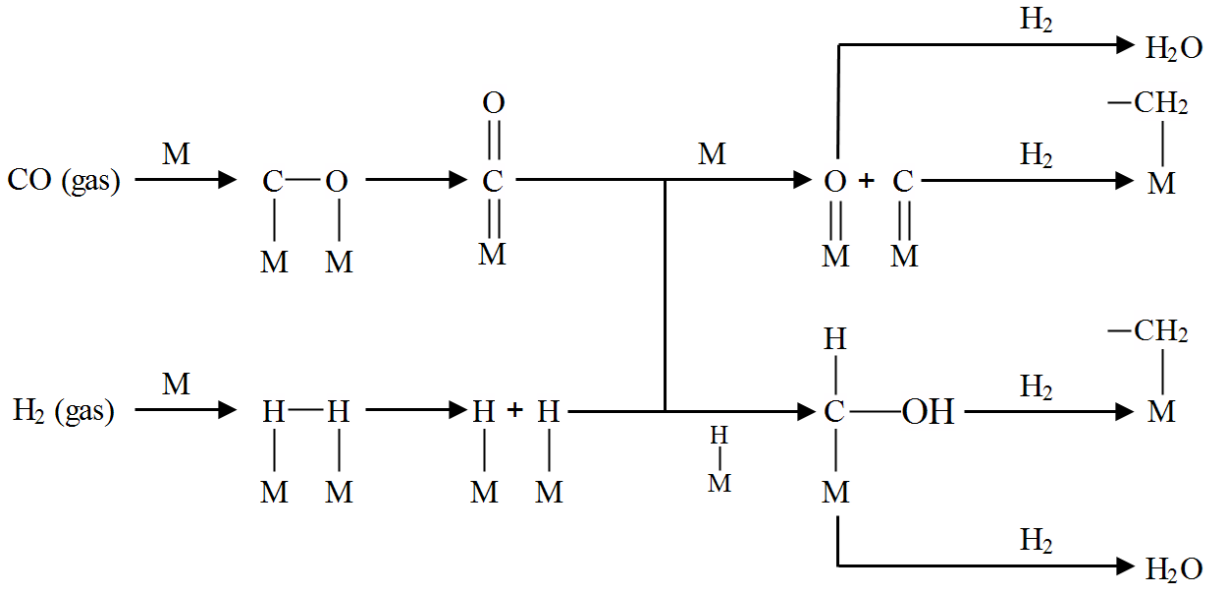

Figure 5: Initiation step in carbide mechanism during Fischer-Tropsch synthesis reaction [27]

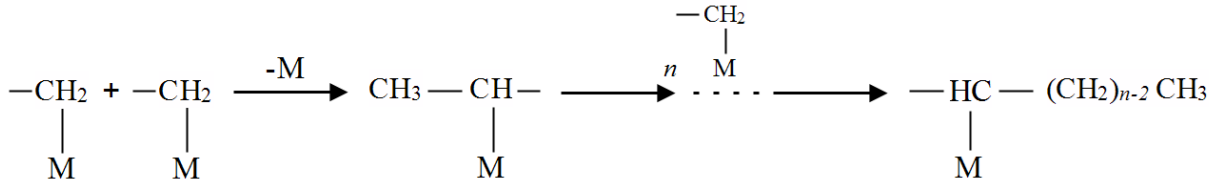

Figure 6: Chain propagation of monomer units in carbide mechanism during FTS process [9, 27]

ide is adsorbed more forcefully than the hydrogen on the catalytic surface sites [26]. C_1 intermediate species (M-CH_x) are formed during the reaction of surface carbon with chemisorbed surface hydrogen atoms. The hydrogenation of surface C atoms of metal carbides to surface CH_2 (methylene species) removes the oxygen as water; which was the probable path in the original mechanism assumed by Franz Fischer and Hans Tropsch in 1926 [27]. The reactions of the adsorbed oxygen with the adsorbed hydrogen lead to the elimination of the oxygen from the surface metals. Figure 5 illustrates the initiation step in a carbide mechanism with two different paths.

The second plausible path to form the monomer units is the formation of enol groups during the reaction of adsorbed CO with surface hydrogen. The hydrogenation of surface enol groups result in the formation of methyl groups. The hydrogenation of surface enol eliminates the oxygen as water products (Figure 5). Once the initiation occurs, different routes could govern the propagation and chain termination in the synthesis process to produce hydrocarbon molecules. A high temperature F-T reaction condition favours the reaction to follow the first path and a lower F-T reaction temperature causes the oxygenation of the enol groups with a further reaction [23].

Afterwards the chain growth step takes place; when the surfaces M-CH_2 are polymerized by reacting with another M-$CH_2$to form M-CH_2-CH_2-M intermediate. The insertion into the M-CH_2 bonds and subsequently desorption and hydrogenation yields the cycloalkane and cycloalkanes respectively; which explains the formation of cyclic aliphatic hydrocarbons in F-T synthesis [26]. The insertion of CHx groups into the metal-carbon bonds are the proposed the long chain hydrocarbons. The propagation of monomer units has been shown in Figure 6.

The chain termination (Figure 7) occurs by hydrogenation of adsorbed surface alkyl groups (-HC- $(CH2)_{n-2}$-CH_3) to produce paraffins, or during the combination with adsorbed surface CH_3. Olefin products (alkenes) are formed through the β-elimination of the hydrogen from surface alkyl groups with an empty surface site [23].

CO insertion into the metal-carbon bonds summarizes the general chain growth pattern of the CO insertion mechanism in the FTS process. The CO insertion into the M-H bond initiates the F-T reaction in this mechanism. The

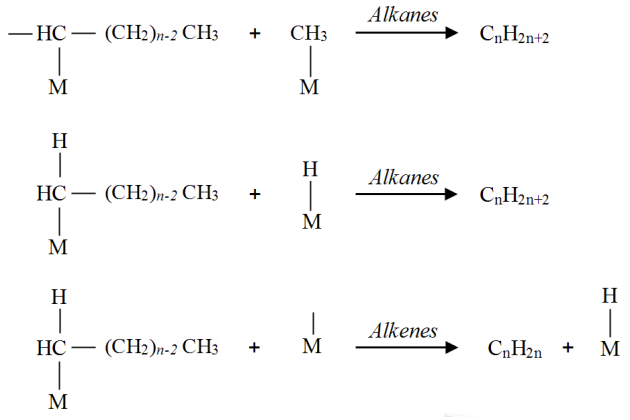

Figure 7: Schematic drawing of the most likely paths in termination step in carbine mechanism for formation of alkanes and alkenes [23]

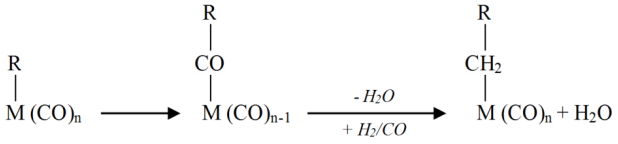

Figure 8: General chain growth pattern in CO insertion mechanism, R represents H or alkyl group [28]

chains are grown by the insertion of carbon monoxide into the metal-alkyl bonds in homogeneous catalysis followed by reduction of the acyl group. The hydrogenation of the resulting acyl groups governs the termination of oxygenates or different hydrocarbons [28]. This mechanism is demonstrated in Figure 8.

The third developed mechanism of F-T synthesis is known as the hydroxycarbene mechanism (Figure 9). This mechanism is based on the formation of hydroxycarbene (CHOH) intermediates. Hydrogenation of chemisorbed carbon monoxides on the metal surface by chemisorbed atomic hydrogen form hydroxycarbene. The water elimination through the condensation of two hydroxymethylene groups forms the C-C bonds. The chain is grown by the cooperation of oxygenated surface intermediates [28].

The reaction for methane formation as an undesirable product in F-T synthesis can be summarized as follows. This reaction is considered as an irreversible and separate reaction. Methane formation (equation 8) increased with increasing of the temperature of the process, so controlling of the reactor temperature and exothermic reaction heat removal are significant considerations of F-T reactor design [29].

$$\text{Methane Formation :} \quad CO + 3H_2 \rightarrow CH_4 + H_2O \qquad (8)$$

The other important reaction that occurs in the FTS process is Water Gas Shift (WGS) reaction that produces water as co-product; this reaction plays a significant, role especially in the reactors in which reactions take place over an iron-based catalyst and produce carbon dioxide as an unwanted product. In general, a higher ratio of H_2/CO forms more H_2O, otherwise CO_2 is formed [30, 31].

$$\text{Water Gas Shift :} \quad CO + H_2O \leftrightarrow CO_2 + H_2 \qquad (9)$$

Sølvi Storsæter *et al.* [32] developed a micro-kinetic model for formation of C_1 and C_2 species over supported cobalt catalysts in Fischer-Tropsch synthesis. The formation of methane, ethane and ethene were proposed within two sets of elementary reactions based on carbon monoxide hydrogenation and hydrogen assisted dissociation of carbon monoxide. These two sets of reaction patterns were combined and a micro-kinetic model was constructed. The activation energy, pre-exponential factors and rate constant were calculated for the elementary reactions involved in carbide and CO insertion mechanisms. The study concluded that the main part of carbon monoxides were converted and subsequently propagated, yielding C_2 products through the CO insertion mechanism and insertion of carbon monoxide into the metal-methyl bonds, respectively. The mechanism of the Fischer-Tropsch synthesis' reaction as well as carbon monoxide activation and methane formation over a supported cobalt catalyst, were studied by Marton Kollar *et al.* [33] and Jia Yang *et al.* [34] respectively.

Rofer-DePoorter [35] performed a comprehensive investigation on Fischer-Tropsch synthesis reaction mechanisms, to bring forward the definition of the Fischer-Tropsch synthesis as the catalytic polymerization and hydrogenation of carbon monoxide to produce heavy hydrocarbons, as well oxygenated products. The elementary reactions within different mechanisms which take place in F-T synthesis have been described in this study. The study was focused on heterogeneous F-T catalytic mechanisms. The production of the side-products, carbon dioxide and water has been discussed. In addition, the paper provides the mechanism of the methanation reaction as a part of F-T synthesis.

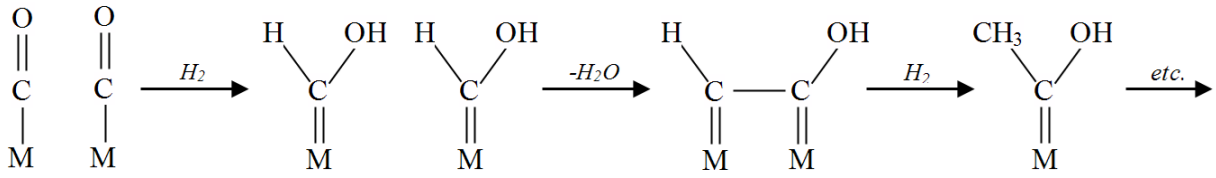

Figure 9: Mechanism scheme of hydroxycarbene intermediates' formation and chain growth pattern during F-T synthesis [28]

4 Amorphous silica surface chemistry

4.1 Introduction of silica materials and general forms

The term silica refers to a large variety of naturally occurring abundant materials in minerals (quartz and flint). Moreover, silica is founded in plants such as rice and bamboo. The general formula for silica is SiO_2 or $SiO_2 \cdot xH_2O$. Synthetic silica is mostly employed in the case of chemical application. The change in preparation conditions such as hydration degree, pressure and temperature could form different phases of silica. The increase of the temperature from 870°C to 1470°C at atmospheric pressure transforms the crystalline phase of quartz from its natural form to be classified in a cristobalite phase (high-temperature polymorph of SiO_2). Amorphous vitreous silica glass is formed at 1700°C [36]. Reaction 10 describes the transformation steps in which different phases of silicas are formed via heat treatment.

$$\text{Quartz} \xleftrightarrow{870^\circ\text{C}} \text{Tridymite} \xleftrightarrow{1470^\circ\text{C}} \text{Cristobalite} \xleftrightarrow{1700^\circ\text{C}} \text{silica glass} \quad (10)$$

The outer surfaces of the crystalline particles participate in any physical or chemical interactions. Accordingly, the specific surface area of the active phase is similar to the geometric surface of silica in the crystalline form involving a high degree of ordering in a dense structure. The fabrication of amorphous silica forms sols, gels, fibres, sheets and powders based on their application. The specific characteristics of silica's texture (surface area, pore diameter and pore volume) are controlled during the preparation in which the physico-chemical behaviour of silica is governed. The amorphous form of silicas with a high degree of porosity could provide a large surface-to-mass ratio. This particular feature of silica makes it more and more attractive for chemical utilizations. The synthetic silicas are classified into the colloidal silica (silica sols) and silica gels (hydrogel, xerogel and aerogel) [36].

4.2 Silica surface structure (physisorbed water, silanol groups and siloxane bridges)

Understanding of silanol functional groups in silicon chemistry could lead to a comprehension in dehydration (removal of physically adsorbed water (physisorbed) and structurally bound water (chemisorbed)), de-hydroxylation (removal of the surface OH groups) and re-hydroxylation mechanisms of silica surface. The hydroxyl groups (≡ Si-OH) over the silica surface are made via valence bond between OH groups and both Si atoms on the surface and in some cases inside the silica's particles with the connectivity of Si-O-H [37]. Many of the chemical and catalytic characteristics of silica depend on the chemistry and geometry of its surface. Therefore, silica surface chemistry was the subject of a number of intensive investigations on molecular adsorption on silica's surface by using an infra-red spectroscopy experimental technique to determine the practical exploitation of this support [38]. Sheppard [39] proved the existence of hydroxyl groups on the SiO_2 surface (porous glass) in various location types in his investigation about chemisorption system and physical adsorption. The presence of silanols on the surface of silica was proven for the first time in Yaroslavsky and Terenin's [37] investigation by employing the infra-red spectroscopy technique.

The course of silica synthesis and re-hydroxylation of de-hydroxylated silica are two principal processes to form the silanol groups on the amorphous silica surface (shown in Figure 10). The silanols' group within the first method are formed during the condensation-polymerization of $Si(OH)_4$. Spherical colloidal particles which contain the hydroxyl groups are formed via the conversion of a supersaturated acid solution into its polymeric form. Finally, surface silanols are created by heat treatment of hydrogel which yields the xerogel. The water or aqueous treatments of de-hydroxylated silica form the surface silanols via the re-hydroxylation process. Within this method, the free valence of surface silicon atoms with complete tetrahedral configuration becomes saturated with OH groups. The condensation of silanols under a specific condition

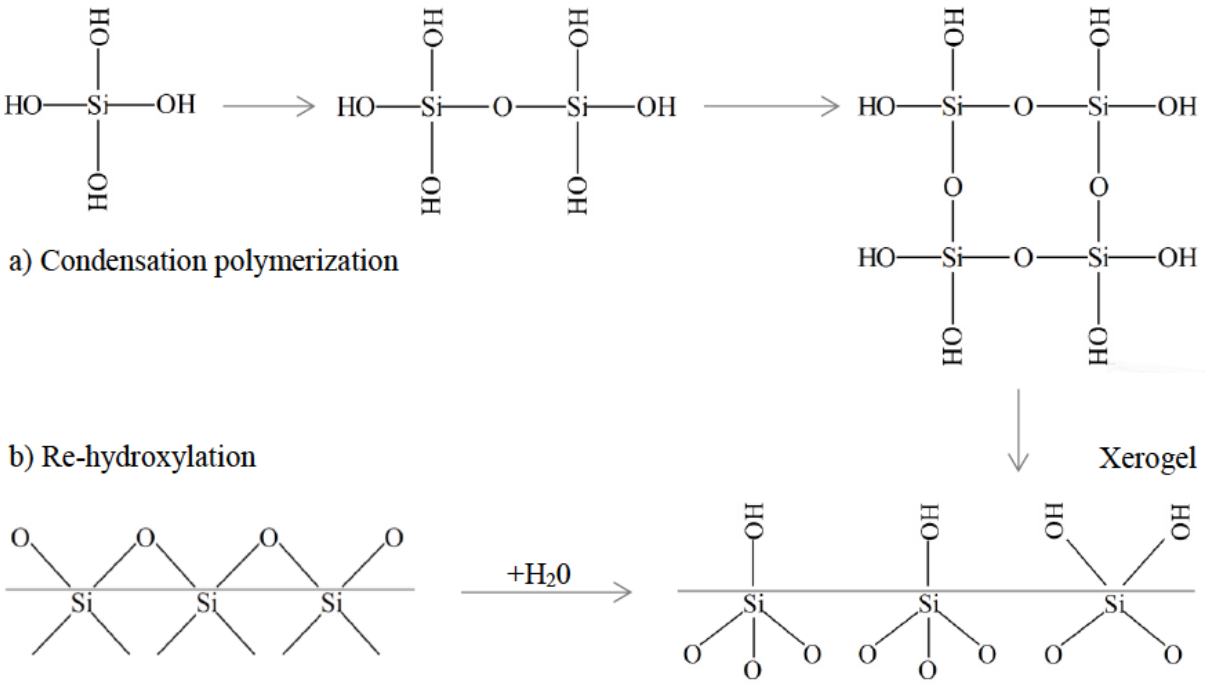

Figure 10: Condensation-polymerization (a) and re-hydroxylation of de-hydroxylated silica (b) processes to form hydroxyl groups on the surface of SiO_2 [37]

form siloxanes bridges (≡ Si-O-Si≡). The formed silanols with hydrophilic features specify the surface properties of amorphous oxide adsorbent silica. The removal of surface hydroxyl groups which are considered as strong adsorption sites, gives the property of being more and more hydrophobic to the silica surface because of the existence of siloxanes [37].

Different kinds of silanols exist on the surface (external silanols) and even throughout the particle structure (internal silanols) of amorphous silica with a porous structure. The internal or intra-globular silanols are not accessible to water. Although there is no clear distinction between the silanols located on the surface with those internally located [36]. The study of Davydov *et al.* [40] showed that the concentration of internal silanols in silica de-hydrated at 200°C was about 0.5 mmol/g. According to the same study no internal hydroxyl groups were reported for silica treated thermally at higher than 600°C.

The existing silanol groups over silica's surface are classified based on their nature, association and multiplicity of sites. The numbers of bridging oxygens (Si-O-) bonded to the central silicon site in different categories are varied from 0 to 4. The single silanols with an OH group are the most preferred hydroxyls over the silica surface. This kind of silanols allocate an OH group per one surface Si atom and are the most probable compounds on a fully hydroxylated silica surface. This category of silanols is known as free or isolated silanols as well, which are located far from neighbouring hydroxyl groups. The isolated silanols are too far from the neighbouring hydroxyl groups, so the formation of hydrogen bonding is prevented. Three bridging oxygens from the bulk structure are bonded to the central silicon site in the free silanols [41]. Figure 11 illustrates schematically the different types of silanol groups and siloxane bridge presented on the surface of amorphous silica.

The silicon sites which are bonded to two bridging oxygens and consist of two hydroxyl groups ($Si(OH)_2$) attached to the silicon atom, are classified in geminal or silanediols silanol group. Peri [42] proposed the existence of geminal groups over the silica's surface for the first time. He concluded that de-hydrated surface structure of cristobalite at 400°C includes about 95% geminal hydroxyl groups. In addition about 85% of de-hydrated silica surface at 600°C was geminal hydroxyl groups. The geminals were close enough to hydrogen bond to each other [36]. It is now agreed that the relative contribution of the geminals on the silica's surface is relatively small to the total number of silanol groups. Morrow [43] observed that a small quantity of silicon atoms on the silica's surface (less than 5% of the total concentration of silanols) treated at 700°C carried out geminal silanols; while most of the silicon atoms

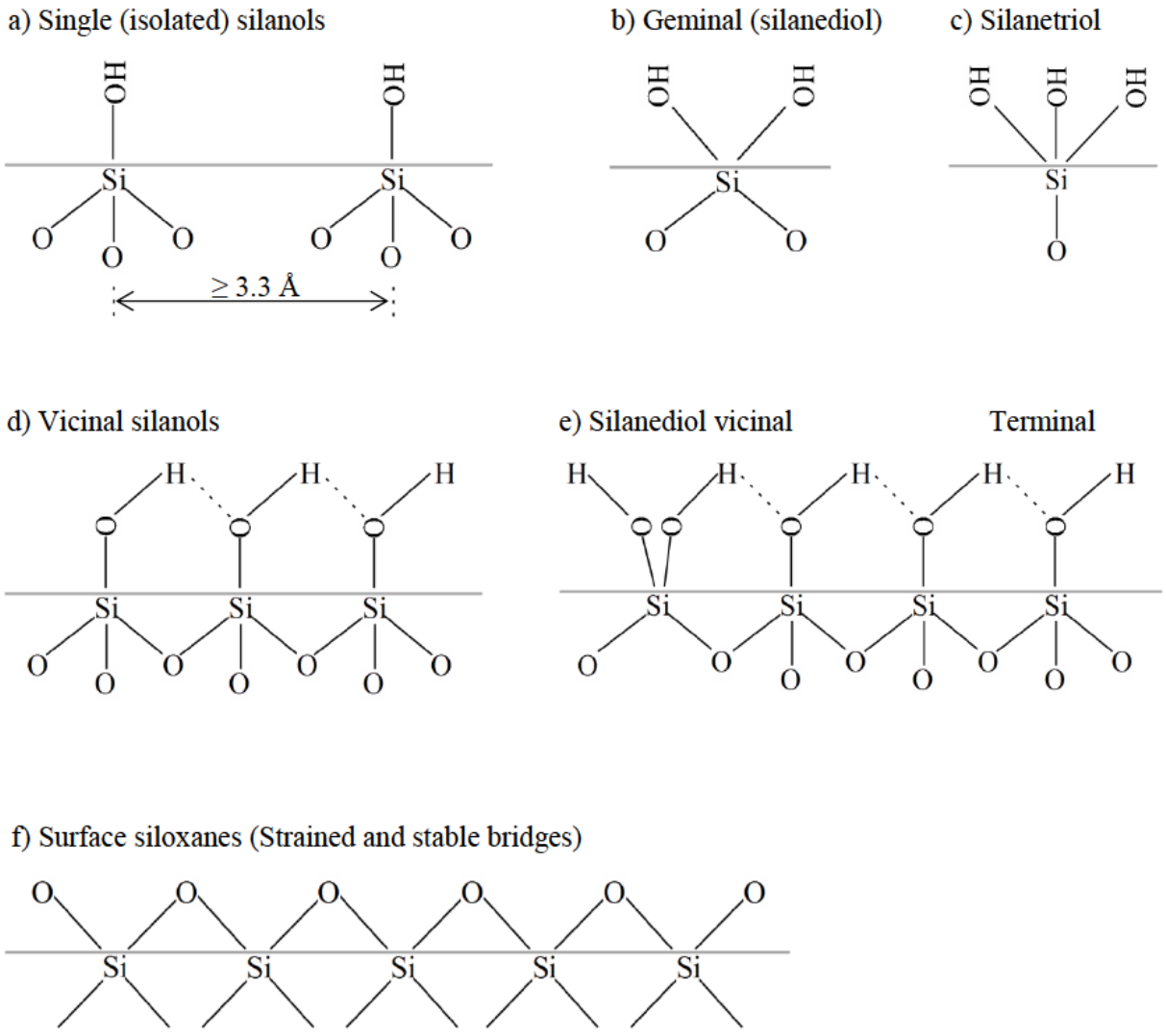

Figure 11: Representation of different silanol groups (isolated, silanediol and Silanetriol silanols), H-bonded silanols (single and silanediol) alongside siloxanes bridges on the surface of colloidal silica [42]

carried single hydroxyl groups being either free or vicinal silanols.

When Si-OH groups are located a sufficient distance from neighbouring hydroxyl groups, the hydrogen bonding occurs between OH and O. These silanols are classified as vicinal or H-bonded silanols. The silanediols silanol are probably bonded to a neighbouring vicinal silanol through a single siloxanes bridge. The result of this bonding is a very weak H-bonded pair. The internal silanols, which in some cases are considered as structurally bonded water, form about 20 percent of the presented silanols in a hydrogel. These groups of silanols are within the structure of the colloidal particles. The heat treatment between 600–800°C causes the condensation of internal silanols. At higher temperature the internal silanols' complete evolution occurs [41]. Siloxanes' bonds are formed through the condensation of internal and surface silanol groups. According to Equation 11, the de-hydroxylation (condensation) process is accompanied by the water formation [36].

$$(\equiv Si - OH) + (\equiv Si - OH) \xrightarrow{\text{Condensation}} (\equiv Si - O - Si \equiv) + H_2O \quad (11)$$

The thermally induced condensation of hydroxyl groups at about 500°C form the strained siloxane bridges. Stable siloxanes groups are the result of the conversion of strained siloxane groups at higher temperature. Both stable and strained siloxane groups are re-hydroxylated upon exposure to water. While it is the case that the re-hydroxylation rate of stable siloxanes are much slower than strained siloxanes. As an example, it takes about

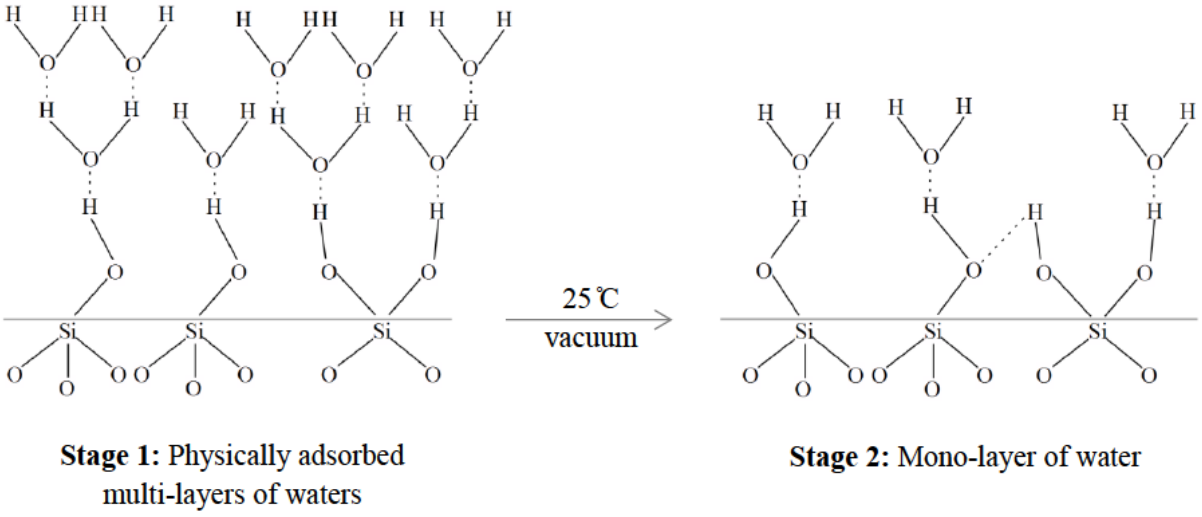

Figure 12: Multi-layer physically adsorbed water de-hydration process, transition from stage 1 to 2 [37]

5 years to completely re-hydroxylate the wide pore silica which is calcined at 900°C. Moreover, the strained siloxanes could completely be re-hydroxylated upon exposure to water [41].

Water molecules are adsorbed mainly to the OH groups of silica's surface. The hydrogen bond between hydrogen and highly electronegative oxygen is associated to any surface/internal silanols type. Due to the highly disordered surface structure of amorphous silica, a regular arrangement of silanol groups is not expected on the silica surface. Irrespective of what kind of hydroxyl groups exist on the surface, a fully hydroxylated surface can be achieved by complete surface coverage. When a porous silica surface is exposed to water at high partial pressure, the capillary condensation takes place on the adsorbed multilayer of water by means of hydrogen bonding, which gradually fills the pore volume by liquid water. The increase in partial pressure of water results in adsorption of a multilayer of water in a fully hydroxylated non-porous silica species as well [36].

4.3 De-hydroxylation and re-hydroxylation of the silica surface

Different treatments at different stages determine the concentration of hydroxyl groups on the silica surface. Physisorbed water de-hydration is an essential process to achieve a successful modified surface. Figures 12 to 16 indicate the silica surface physico-chemical model via heat treatments at different stages during the preparation process. Two types of molecularly adsorbed water have been established formerly (shown in Figure 12). Each of them is de-hydrated at various thermal sub-regions. The first de-hydration stage corresponds to poly-molecular adsorbed water; while the second relates to de-hydration of the monolayer of molecularly adsorbed water on the silica surface [44]. Desorption process of the first stage assigns much lower activation energy than that of the second stage; while the majority mass of the hydrogen-bonded waters are removed at the first stage. The sharp increase in activation energy of the desorption process from stage one to two corresponds to practically complete removal of the monolayer of waters which have been physically adsorbed. Both stages are greatly influenced by the size and morphology of the porous silica as well as its porosity [36].

As shown in Figure 12, at the initial stage, the silica surface is at its maximum state of hydroxylation. Multilayers of water have been adsorbed physically, which covers the silica surface containing different kinds of silanols (isolated, geminal and vicinal silanols). The H-bond networks alongside the water multi-layer cover the surface OH groups. At this stage, internal OH groups inside the silica skeleton exist. Transition to the second stage at 25°C removes the multi-layer of water. Thereupon, a single layer of physically adsorbed water is retained at this temperature. This stage is easily reversible to the first stage upon the exposure of water. Figure 12 (stage 2) indicates the mono layer or less of the physisorbed water on the silica surface, which is retained on the surface at temperatures less than 180°C [37].

Transition from stage two to three (Figure 13) results in complete removal of strongly physisorbed water. The threshold temperature for the complete de-hydration is es-

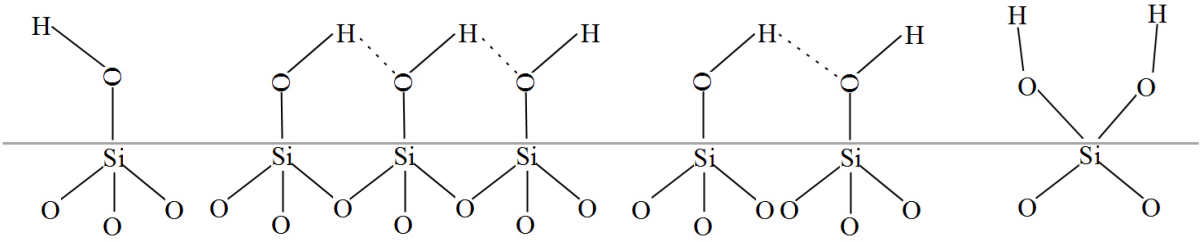

Figure 13: Complete removal of physisorbed water to achieve a dry silica surface (transition from stage 2 to 3, 180°C ≤ T ≤ 200°C) [37, 45]

timated to be at 190 ± 10°C. The re-hydroxylation stage is begun by completion of the de-hydration stage. Both of the stages, de-hydration and de-hydroxylation are very heterogeneous processes [45].

Zhuravlev [44] applied temperature-programmed desorption (TPD) experiments by employing the mass spectrometric thermal analysis method to investigate the dehydration and de-hydroxylation of the silica surface. He concluded that more physisorbed water coverage on the silica surface leads to a higher activation energy of water desorption process in the transition from stage one to two, as well as from the second stage to the third stage. The silica surface's behaviour at the introduction of water is the same as stage two.

The next stage is to condense the vicinal groups by further heat treating at about 450 to 500°C. At this stage, the average distance between the neighbouring free hydroxyl groups are increased over the silica surface, which causes a decrease in the de-hydroxylation process. The heat treatment of the silica surface at this stage releases water vapor. The resulting silanol groups of this stage consist of singles and geminals. The resulting surface coverage of silica at this stage has been shown in Figure 14, a). The numbers of isolated silanols are increased as a result of the transition from stage 3 to 4 by thermal treatment between 200 to 400°C. The acid treatment of silica could result in a higher concentration of silanols over the silica surface as well [46]. On the other hand, the number of isolated silanols could be decreased by the re-hydroxylation process, which increases the concentration of bonded silanols. With completion of the transition phase, further heat treatment at this stage decreases slightly the concentration of the silanols. The porous structure of the silica support could accelerate the de-hydroxylation process. For the silica with wide based pore structure, a decrease in the number of bridged silanols occurs at a higher temperature than for that with smaller pores [45]. As the temperature is relatively low, the siloxanes remain in a strained bridges state. In some cases, the complete re-hydroxylation occurs when the weakened strained siloxanes' bridges are split. The estimated ratio of isolated/geminal silanols is about 85/15 at this stage. The condensation of internal silanols occurred at about 600–800°C; at this temperature the concentration of isolated and geminal silanols decrease respectively. At about 800 to 900°C, the silica skeleton becomes free of internal OH groups as well as the geminal silanols disappearing completely from the silica's surface. Stable siloxane bridges are formed in considerable numbers while isolated silanols remain on the silica surface (shown in Figure 14, b). When the silica surface is covered by the stable siloxane, the OH groups' concentration is decreased, which leads to a sharp increase in activation energy of the de-hydroxylation process. The concentration ratio of OH group to siloxane bridges determines the hydrophilic or hydrophobic property of the silica surface. Re-hydroxylation at this stage hardly takes place at room temperature. The hydrophilic characteristic of the silica surface continues to decrease till the surface is covered entirely by Si-O-Si groups and Si atoms which make the surface fully hydrophobic.

Different types of hydroxyl groups (bonded and isolated silanols) possess different activities of adsorption. The isolated silanols are considered to have more reactivity and adsorption activity than that of H-bonded silanols. The vicinal (H-bonded) silanols are formed in a linear or two-dimensional structure. In such a structure of hydroxyl groups, probably at least more than two silanols are engaged. In that case, less re-active hydrogen, even in some cases no more re-active hydrogen, would be available due to the involving of the hydrogen in H-bonding in the vicinal groups' structure, which does not form pairs [45]. Figure 15 indicates the re-active hydrogen over the silica surface.

Transition from stage four to five (T ≥ 1200°C) results in complete removal of OH groups and full coverage of the silica surface with Si-O-Si groups. At this stage, the surface of SiO_2 only consists of siloxane bridges [37, 41]. Figure 16 indicates the thermal removal of silanols as a result of siloxanes' formation.

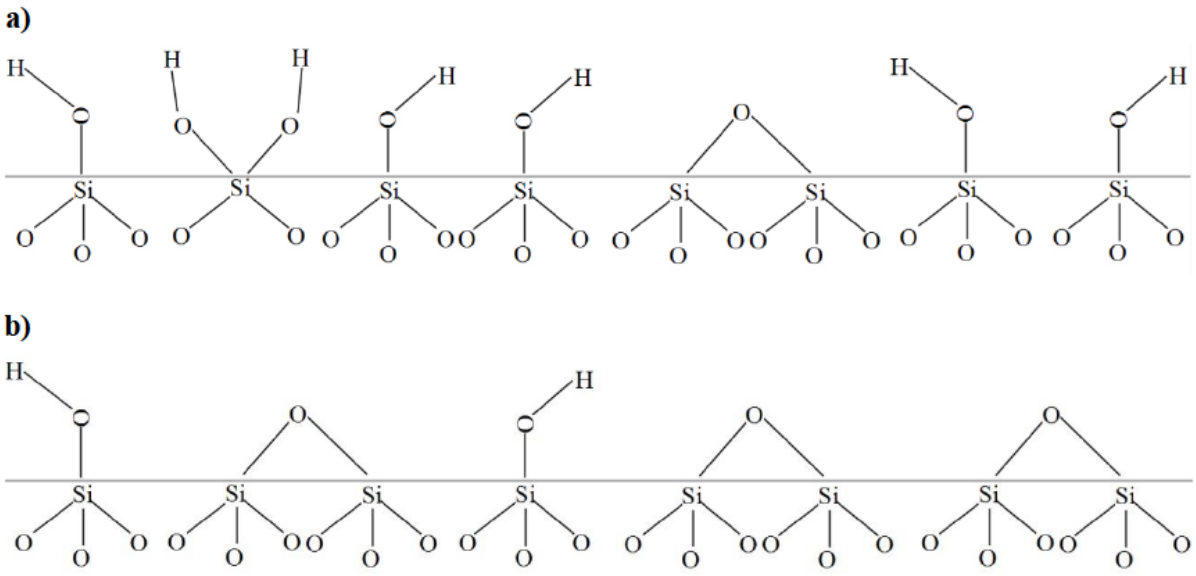

Figure 14: Condensation process of silica surface by heat treatment, transition from stage 3 to 4 (stage 4a: 450°C ≤ T ≤ 500°C, stage 4b: 8000°C ≤ T ≤ 900°C) [9, 45]

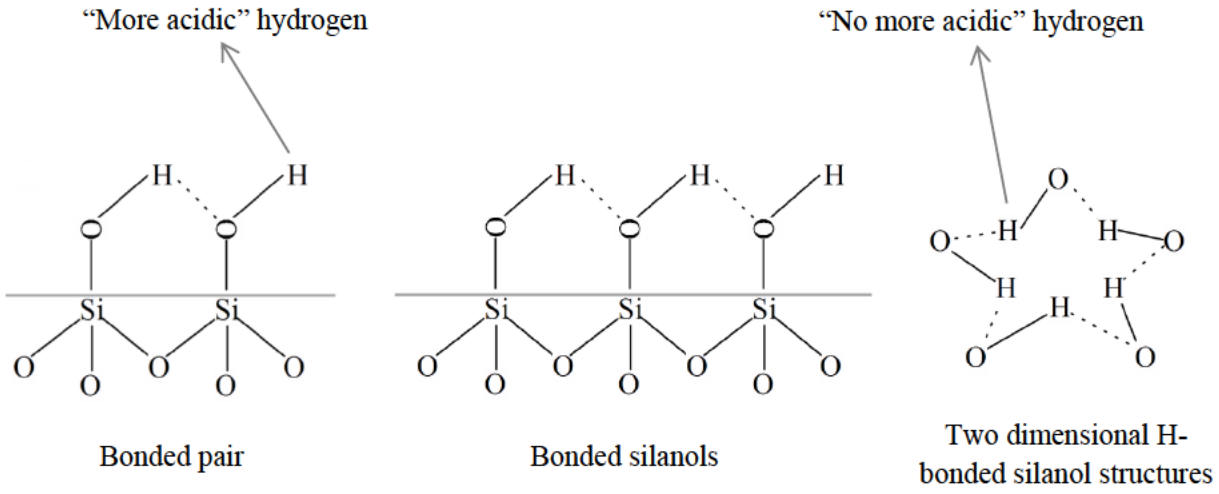

Figure 15: H-bonded silanols on the silica surface, acidic and no acidic hydrogens [45]

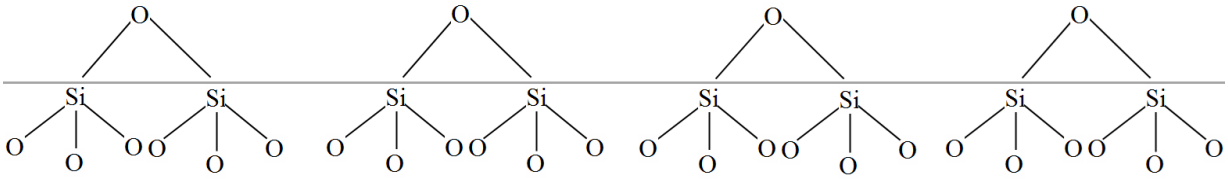

Figure 16: Fully de-hydroxylated surface of silica, transition from stage 4 to 5 (1200°C ≤ T) [37, 41]

Bermudez [47] achieved complete de-hydration of a silica surface at 100°C. At this temperature the de-hydroxylation of some silanols was observed as well. Hail [48] concluded that the major adsorptive property of the silica surface corresponds to surface hydroxyl groups, according to that study, by using infra-red gravimetric adsorption. The adsorption sites could be either freely vibrating or hydrogen-bonded to each other depending on the pre-treatment and temperature. The chemical re-activity of the silanol groups on the silica surface were affected by a

small amount of impurities. Voort [49] revealed weak surface heterogeneity on silica gel by the contribution of free and bridged hydroxyl groups. The investigation was carried out by using the temperature-programmed desorption (TPD) experiment via strong hydrogen-bonding interaction between surface hydroxyl groups (free and hydrogen-bonded) and the adsorbed pyridine molecule. Various energetic sites were observed. The observed activation energy of pyridine desorbed from free hydroxyl groups was higher than that of bridged hydroxyls. It was concluded that the bridged silanols were de-hydroxylated much easier than isolated silanols.

Chuang *et al.* [50], in their investigation, considered the participation of different hydroxyl groups in hydrogen-bonding or either non-hydrogen bonding, depending on surface segment type, relative hydroxyl groups orientation, as well as their local structural environments. They performed this study based on a generalized β-cristobalite surface model of silica. The de-hydroxylation temperatures and conditions of isolated and geminal silanols were considered in this study. In addition, yielding of highly strained siloxanes through de-hydroxylation at a higher temperature was also examined. The model enabled the explanation of de-hydroxylation/re-hydroxylation processes as well as re-hydration/de-hydration behaviours of the silica surface which take places under specific conditions.

5 Catalyst formulation and reaction engineering in the F-T process

5.1 F-T catalyst formulation

The product selectivity in F-T synthesis can be varied over a wide range. Catalyst formulation, the system which performs the synthesis process and reaction conditions, is the key factor that affects the product distribution in F-T synthesis. Chain growth probability (α) in F-T synthesis is influenced by the catalyst selected for the hydrogenation process. In addition to catalyst type, the chain growth probability mechanism on the catalyst surface is affected by the catalyst's promoter level and temperature and composition of feedstock gas as well. It should be mentioned that the probability of the chain growth is independent of both the chain length and reactor type [51]. Cobalt, iron, ruthenium and nickel are considered as commercial catalysts in bio-fuel generation. These metals in their metallic form have the capability like all elements of VIII B group in the periodic table [52] to dissociatively adsorb carbon monoxide to form metal carbide on the catalytic surface and hydrogenate the adsorbed carbides. Ruthenium is not of interest for commercial application because of its high cost; despite the fact that it is one of the most active catalysts for F-T synthesis. Nickel does not have industrial relevance in F-T technology. The low average molecular weight of nickel prevents the usage of this metal for the F-T process. The small particle size of nickel leads to higher hydrogenation activity power compared to its chain growth power [52] Water Gas Shift (WGS) reaction activity over an iron catalyst in the F-T process is more than that of cobalt, which can lead to loss of carbon monoxide as a raw material by the formation of carbon dioxide. The activity of the WGS reaction produces more water as a co-product of this process, which is the kinetic inhibition of an iron catalyst. On the other hand, the higher activity of the WGS reaction over an iron catalyst allows the utilization of synthesis gas which contains carbon dioxide or hydrogen depleted syngas [53]. A cobalt-based catalyst is of interest for industrial applications due to its significant specifications. The high selectivity of a cobalt catalyst to long chain alkanes, its low selectivity to oxygenate products and alkene as well as high deactivation resistance, long-life time and the relatively low price of this catalyst make it appropriate to be utilized for F-T biodiesel generation [54]. A cobalt-based catalyst is an efficient and capable catalyst due to its high activity at low temperature [14]. In addition, a cobalt catalyst has durability of up to 5 years on stream compared to 6 months in the case of an iron catalyst [53]. A cobalt catalyst generally yields in higher production of long-chain synthetic hydrocarbon [21]. The FTS process over a cobalt catalyst at normal pressure and temperature of 200–300°C produces linear olefins (α-olefins) as the main products. A small amount of non-linear products consisting mainly of mono-methyl branched compounds are produced at this temperature. High pressure Fischer-Tropsch Synthesis over a cobalt catalyst produces less olefins in favour of an alkanes' content due to the increase of molecular weight [28]. Chain growth probability is 0.5-0.7 for an iron catalyst and 0.7-0.8 for a cobalt catalyst. Chain growth probability can be maximized up to a value of 0.95 for a cobalt catalyst. It works well when the H_2/CO ratio is near to two [53].

Fischer-Tropsch synthesis in an iron-based fixed-bed reactor produces naphthenes and aromatics in small amounts; it is the case that cobalt and ruthenium-based fixed-bed reactors usually produce none of these compounds [27]. In comparison with iron and ruthenium catalysts, cobalt has a low rate of carbon monoxide activation, while low hydrogenolysis and low shift activity at a high H_2/CO ratio make it reasonable for synthetic diesel

production (Fe < Co < Ru). This catalyst has high hydrogenation activity when alkanes are preferred as the main product (Ru > Co > Fe). The cobalt-based catalyst is not affected by steam practically in the F-T reaction regime [55].

5.2 Catalyst carrier materials

Support material and its nature are relevant significant parameters that influence the catalytic activity and products' selectivity in F-T synthesis. Metal-support interaction strength, resistance to attrition (mechanical properties), thermal stability and support's porosity are the features that influence the reaction and transfer phenomenon in the F-T process. Diffusion limitation for reactant and produced hydrocarbons caused by catalyst liquid-filled pores and capillary condensation of heavier hydrocarbons, influence the overall F-T reaction rate [56]. Under F-T synthesis conditions, the pores are filled with liquid/wax products. The reactants at the external surface of the catalyst dissolve in the waxes. The dissolved reactants diffuse inside the pores through the wax. Hydrogen possesses a higher diffusion coefficient compared to carbon monoxide. These phenomena result in a higher concentration of hydrogen inside the porous catalyst. The increase in H_2/CO ratio accelerates the chain termination step and negatively affects the product selectivity and chain length of the products by pore diffusion limitation [57]. Usage of an eggshell catalyst in the F-T process could enhance the desired product selectivity by decoupling the severe transport restriction.

In addition to all the above mentioned, the properties of metal particles' size and active phase dispersion are considered to be affected by the pore size located inside [56]. Catalyst support plays a significant role in the catalytic behaviour of supported metal by changing the charge and size of metal particles, the particle shape and crystallographic structure, as well as the formation of active sites [58]. Saib *et al.* [59] studied the effect of support pore diameter on the performance of F-T synthesis and observed different adsorption properties of cobalt particles and cobalt crystalline size located in narrow and wide pores. Different types of metal oxide supports such as aluminium oxide (Al_2O_3), silicon dioxide (SiO_2), titanium dioxide (TiO_2), or zeolite are employed as the carrier of catalyst materials, especially when the active sites are more expensive, like cobalt.

Combinations of remarkable characteristics such as large surface area, high surface/mass ratio as well as ultra-low density of silica, make it a marvellous support for F-T catalyst preparation. The high porosity degree of silica, its pores network and open pores volume rather than bulk volume, make it an attractive candidate for F-T catalyst support. This support facilitates the internal mass transfer due to its interconnected three dimensional networks which could form up to 99.8% of its bulk volume [60]. The application of eggshell distribution of a catalyst could result in faster diffusion of higher molecular weight hydrocarbons, due to the deposition of an active phase in the outer region of the catalyst's pellets. This distribution of the catalyst lowers the intra-particle mass transport and yields to higher selectivity of middle distillate hydrocarbons [61] which are the desired products of this investigation. In addition, cobalt is highly active compared to iron, nickel and ruthenium when supported with silica, due to the fact that the nature of the support affects the catalyst's behaviour [62].

Gaderzi *et al.* [63] examined the effect of calcination conditions on the performance of a cobalt/silica catalyst and also considered the metal crystallites distribution affected by solvent, during catalyst preparation via solution impregnation; they achieved higher active surface area and better dispersed metal, in the case of alcohol as a primary solvent compared to water. Song *et al.* [64] considered the effect of support pore size on catalyst characterization and its activity in the F-T hydrogenation process; and concluded higher activity and productivity for the catalyst with pore sizes ranging 6–10 nm. Girardon *et al.* [65] studied the effect of a cobalt precursor impregnated to silica support via incipient wetness impregnation and achieved higher active site concentration and catalytic activity for the catalyst prepared by cobalt nitrate. Zhang *et al.* [66] observed the best catalytic performance for the cobalt catalyst supported by silica gel prepared from dehydrated ethanol. The application of absolute ethanol resulted in a decrease in solvent polarity as well as prevention of the formation of an immobilized glassy water layer. As a result, higher interaction between more cobalt complex and the silica gel surface was provided. In that case, formation of highly dispersed small particles of cobalt species was obtained; these particles were activated at higher temperature.

Jae-Sun Junga [67] showed in his work that pore diameter and pore size distribution, which depends on the mesoporous support structure affects the cobalt particle size and significantly influences the catalytic activity of a cobalt catalyst in the F-T hydrogenation process. Anna Maria Venezia [68] enhanced the activity of a sol-gel prepared silica supported cobalt catalyst by adding a small amount of titania which was examined at different space velocities and high space velocity and resulted in higher Fischer-Tropsch reaction conversion and higher selectiv-

ity of heavier hydrocarbons. Shouli Sun *et al.* [69] was successful in increasing the activity of a cobalt catalyst, supported by silica gel support prepared by incipient wetness impregnation of cobalt (II) nitrate and cobalt (II) acetate employed for F-T synthesis. Yi Zhang [70] applied different solvents (acetic acid and ethanol) to prepare a highly active Co/SiO_2 catalyst for Fischer Tropsch synthesis and reported higher dispersion of the cobalt active site and reducibility, for a catalyst prepared with ethanol solvent; which resulted in higher activity of this catalyst in the F-T process. Hui Ming [71] studied the effect of different rare earth promoters on hydrogenation performance of a cobalt supported silica gel catalyst and realized praseodymium as the most effective promoter.

5.3 F-T reactor technology

Different kinds of reactors are employed to convert syngas to synthetic fuel, such as multi-tubular, slurry bubble column and fluidized bed reactors. Multi-tubular fixed-bed and slurry phase reactors are the types of reactors that are employed for low-temperature (T<530 K) Fischer-Tropsch synthesis [72]. Fixed bed reactor's technology is known as the most efficient reactor to maximize the synthesis driving force of the F-T process in the absence of heat transfer limitations [26]. There are some disadvantages in these reactors. High pressure drop occurs in a fixed-bed reactor and also low catalyst utilization can be achieved. Insufficient heat removal and limited diffusion are two other drawbacks of fixed-bed reactors. A fixed-bed reactor is employed to produce synthetic fuel due to its significant features. The ease of scale up from single-bed to pilot plant, the ease of catalyst loading and replacement are two leading features of fixed bed reactors [73]. F-T reaction is highly exothermic (ΔH_{298K} = −140 to −160 kJ.mol^{-1} CO converted, depending on the products) and produces waste heat that must be removed from the reactor. Heat transfer limitation is a major disadvantage of a fixed bed reactor and may lead to more activity of the methane formation reaction, low product selectivity and a shorter lifetime of the catalyst [74]. Radial heat transfer to the wall of a fixed-bed reactor and cooling medium is one of the aspects which should be taken into account. F-T synthesis is an exothermic reaction which produces waste heat. Nitrogen efficiently removes the produced heat of the exothermic F-T reaction and minimises the temperature's runaway probability. The application of nitrogen in feedstock leads to a cost-effective synthesis process due to the increase in the reactor's tubes diameter [75].

Chambrey *et al.* [74] performed a comparative study of FTS in three different reactors. The results of this research showed higher hydrocarbon productivity for a miliscale fixed-bed reactor, compared to the two other reactors. Slow catalyst deactivation took place in the fixed-bed reactor and 0.92 chain growth probability was obtained. In this investigation, the fixed-bed reactor was employed to maximise the synthesis driving force, which is known as the most efficient reactor technology for synthesis of heavier hydrocarbons in the absence of heat and mass transfer limitations. This reactor produces more hydrogenated, less oxygenated and alkene products, compared to fluidize and slurry bed reactors. There is no restriction in the reaction phase of fixed-bed synthesis [76].

5.4 Overview of previous works regarding the Fischer-Tropsch synthesis process

Gonza´lez *et al.* [77] studied the behaviour of a cobalt catalyst supported on different meso-structured supports based on silica in the Fischer-Tropsch Synthesis process and observed highest activity of the catalyst in terms of carbon monoxide conversion; as well as heavy hydrocarbon product selectivity for the catalyst supported with 5 nm average pore diameter. They concluded that the average pore size of the mesoporous support highly impacted on the reducibility of the cobalt particles by forming a different size of supported cobalt clusters irrespective of higher dispersion.

Osakoo *et al.* [78] increased the activity of a cobalt catalyst supported by SiO_2 by improving the cobalt particle size (using impregnation method) and subsequently its reducibility (by creating larger cobalt particle size); as well as by promoting the catalyst with 0.2 wt% palladium (Pd). They enhanced the formation of alkanes by adding the Pd as the promoter, which resulted in higher selectivity of heavy alkanes, methyl-branched paraffins as well as alcohols. Wu *et al.* [79] concluded from their work that adding a small amount of TiO_2 could enhance the reducibility of a cobalt catalyst supported with silica gel by affecting the support-catalyst interaction and subsequently could result in higher FTS reaction activity. The dispersion of active metal was improved as well by the addition of TiO_2. Khodakov *et al.* [80] examined cobalt dispersion as well as its reducibility affected by the meso-porous structure of silica support (narrow and broad pore sized distribution in silica support) and concluded that the catalytic performance of a narrow pore sized catalyst was better than that of a broad pore size due to higher dispersion of the active site over this support.

Dunn *et al.* [60] concluded the increase in the loading of cobalt content supported with silica aerogel up to 10 wt% resulted in higher activity of this catalyst in the Fischer-Tropsch Synthesis process. Ma *et al.* [81] observed that due to the increase in the density of active Co^0 on the surface site, the average cobalt cluster diameter decreased by about 30% (from 38.4 nm for a catalyst containing 15 wt% metal content to 27 nm for a catalyst containing 25 wt% metal content) in a cobalt catalyst supported by silica, resulted in an increase in the intrinsic reaction rate constant by about 102%. Hong *et al.* [82] enhanced the reducibility and catalytic activity of cobalt supported silica in F-T synthesis by adding organic additive (sorbitol, $HOCH_2(CHOH)_4CH_2OH$) to the impregnation solution during the preparation step. This enhancement was due to stabilizing of Co^{2+} due to the adding of the sorbitol. The sorbitol caused the cobalt complexes to decompose at a higher temperature and therefore higher dispersion in cobalt oxide was achieved.

Gnanamani *et al.* [83] produced hcp (hexagonal close-packed) and fcc (face-centred cubic) cobalt metal particles over silica support by employing different pre-treatments and observed higher carbon cobalt dispersion (5.06% in the case of hcp and 3.84% in the case of fcc) for the catalyst containing the hcp metallic phase; and subsequently higher carbon monoxide conversion (about 28 mol%) was achieved in this study, compared to that of fcc. Since the cobalt catalyst used in Fischer-Tropsch synthesis is expensive, hence, Loosdrecht *et al.* [84] investigated the oxidation of nano-sized metallic cobalt during realistic F-T synthesis to cobalt oxide and concluded that this type of oxidation is independent of the support materials and could prevent the correct combination of reactor partial pressure of H_2O and H_2 (P_{H2O}/P_{H2}). The cobalt crystalline size was 6 nm in this study. Storsæter *et al.* [85] characterized un-promoted and rhenium-promoted cobalt catalysts supported with titania, silica and alumina in Fischer-Tropsch synthesis. This investigation showed a relatively higher activity of a Re-promoted cobalt catalyst when it was supported with TiO_2.

Hunpinyo *et al.* [86] performed a kinetic study in both a laboratory-scale and pilot-scale BTL process using a fixed bed reactor, to examine the performance of a ruthenium-based alumina supported catalyst in the F-T synthesis process at atmospheric pressure; they observed higher activity of this catalyst towards the formation of the desired heavy molecular weight hydrocarbons (CO conversion @ temperature = 220°C and space velocity=3600 hr^{-1}). Similar results in terms of product selectivity as well as distribution of hydrocarbon products were achieved in the cases of both the laboratory and pilot scale BTL processes.

Elbashir *et al.* [87] presented an integrated approach in the designing of an advanced multiphase F-T reactor. Three parameters were identified in order to systemize the designing process, including: (i) process synthesis, (ii) process simulation and (iii) tailored experiments. The process configuration was generated from various building blocks within the process synthesis (*e.g.* reaction, separation, recycling, recovery). The process simulation evaluated the synthesized system performance and finally the generated design was verified experimentally. The study was successful to optimise the F-T reactor technology for near/super critical operation conditions. Guettel *et al.* [88] derived a mathematical model to compare the performance of different types of reactors (fixed-bed reactor, slurry bubble reactor, micro- and monolith reactors) in the Low-Temperature Fischer-Tropsch (LTFT) synthesis process. The lowest specific catalytic productivity in the simulation study was observed for the fixed-bed reactor operating at a trickle-flow regime due to severe resistances in mass transfer. However, the ease of separation of the catalyst from liquid products is still a significant advantage for the fixed-bed reactor to be employed in commercial-scale plant F-T synthesis. Schulz [89] presented a history of the Fischer-Tropsch synthesis process as well as its trends, by generalising some individual investigations including the development of the F-T reactor and process, F-T catalyst formulation, micro kinetic modelling of F-T reactions etc.

Chu *et al.* [90] considered the effect of calcination temperature during catalyst preparation steps as well as platinum (Pt) promotion of a cobalt catalyst supported with alumina on the interaction of metal oxide (Co_3O_4) with support materials. It was concluded that unlike the calcination temperature and promoting material, which had no significant influence in the size of the generated metal oxides crystallite size in the supported gamma-alumina, the particle size and subsequently its dispersion was greatly affected by pore size distribution. The rate of the F-T reaction was significantly increased by promoting the catalyst with a small amount of platinum. In contrast with the reaction rate, a slight decrease in the production of heavy hydrocarbons was observed in this study.

Zhang *et al.* [91] considered the performance of a cobalt-based alumina supported F-T catalyst by modification of the support by magnesia. The performance of the magnesia-modified catalyst was examined in F-T synthesis and it was concluded that the activity of the catalyst in terms of carbon monoxide conversion was increased due to improvement in reducibility of the catalyst. It was observed that the increase in magnesia content resulted in a decrease in catalyst activity, heavy hydrocarbon selectiv-

ity, as well as higher selectivity of co-products; due to the formation of MgO-CoO solution.

Itkulova *et al.* [92] studied the production of ceresin (mixture of high molecular-weight hard hydrocarbons including n- and iso-alkanes) under pilot scale F-T synthesis, using a cobalt catalyst modified with platinum (Pt) and observed that promotion of the catalyst with 0.25 wt% of the second metal resulted in 77% selectivity to ceresin fraction in the reactor output. The liquid synthesis process was optimised in this investigation in order to find the most selective reaction conditions for the production of ceresin. The best combination of cobalt catalyst and fixed bed reactor was found at 170-180°C and space velocity of 100 hr^{-1}.

Schulz [93] performed a comparative investigation on the dynamics of the structure and the function of cobalt and iron based catalysts in Fischer-Tropsch synthesis of liquid hydrocarbons, to obtain a deep understanding of the specific behaviours of these two catalysts in the F-T process. It was concluded that the active sites of a cobalt-based F-T catalyst are of a dynamic nature. Thus, the elemental reaction's relative rates correspond to the time on stream, reaction temperature, and partial pressure of reactants (mainly hydrogen and carbon monoxide), while statics' structural function was observed for the iron-based catalyst, which means the rate of F-T reaction is increased during the catalyst re-assembling (dissociative hydrogenation of carbon monoxide with iron to create active surface carbide); Whereas the selectivity didn't change. In the case of the iron catalyst, the final product's average molecular weight was controlled by a change in temperature, which means that only the temperature parameter had a significant influence.

Jacobs *et al.* [94] performed a comparable work to examine the effect of co-fed water on a cobalt catalyst prepared with variable supports (Al_2O_3, TiO_2, SiO_2). A positive influence of co-fed H_2O was observed for the silica supported cobalt catalyst which resulted in an increase in conversion of carbon monoxide as well as C_{5+} hydrocarbons' selectivity. At the same time, the methane selectivity was decreased while the carbon dioxide selectivity remained low. The rate of catalyst deactivation was accelerated with the increasing of the water content at the inlet. In contrast, the activity of the cobalt catalyst in terms of carbon monoxide conversion was decreased when the metal was supported with TiO_2 and Al_2O_3 with a strong cobalt oxide support interaction.

Pichler *et al.* [28] studied the product composition of the F-T synthesis as a function of residence time on the catalyst at low pressure (normal pressure) and low temperature (200°C) over cobalt/thorium oxide/kieselguhr catalyst ($H_2/CO = 2$) and concluded that the shorter the residence time leads to a larger α-olefin fraction of the product. In addition, it was concluded that at low space velocity, the primarily formed α-olefins are transformed within the secondary reactions into β-olefin, linear paraffins and methyl branched products.

6 Conclusion

At the present, approximately 90 million barrels of crude oil are demanded per day from which about 85 percent is required to produce liquid transport fuels. The contribution of the production of liquid transport fuels via alternative processes such as BTL, GTL and Waste- To-Liquid (WTL) is still less than five percent. Crude oil is not a sustainable source of energy. In addition, it is estimated that within the next half century, countries will face a shortfall in production of crude oil in comparison to the demand of transporting energy. This is one of the consequences of global economy growth, which makes the investigation regarding the alternative sustainable energies very essential. Hence, a huge amount of research is in progress to convert part of agricultural products (lignocellulose biomass), which do not include products suitable for the human food chain into a required liquid fuel. This idea could not solve the country's energy needs but could reduce dependency on crude oil. Fischer-Tropsch synthesis constitutes one of the routes within the indirect liquefaction process. As a result of hydrogenation of carbon monoxide and consequently polymerization of carbide metal, a wide range of products (hydrocarbons, oxygenates and water) are produced with a vast distribution in carbon number.

This paper presented a comprehensive literature review on the Fischer-Tropsch synthesis (FTS) process including a history of production of liquid hydrocarbons through F-T technology; the importance of second-generation bio-fuels in future transporting energy and its advantages as well as the characteristics, of organic materials, which are exploited as feedstock in the F-T process to be converted to long-chain hydrocarbons. In addition, this paper represented the surface polymerization mechanisms for the production of a wide-range of hydrocarbons in the Fischer-Tropsch process. The silanol functional groups are represented as well as the attempt to achieve a comprehension in de-hydration, de-hydroxylation, as well as re-hydroxylation mechanisms of the silica surface. Furthermore, catalyst formulation and reaction engineering in Fischer-Tropsch synthesis are reviewed.

Intensive investigations require in terms of technical development of SGB to ensure the success in deployment

of FT technology. The catalyst deactivation, selectivity towards a narrower product distribution and heat and mass transfer limitation are three main challenges in improvement of LTFT process. Hence, future investigations should advance the research towards considering multi scale approaches for potential improvement in existing problems with LTFT process including (i) active nanoparticles' size, their adjustment and long-term stability in micro scale, (ii) porous support structure, effects of internal mass transfer, diffusion limitation for reactants and produced hydrocarbons caused by catalyst liquid-filled pores and capillary condensation of heavier hydrocarbons in meso scale and (iii) catalyst combination with operating regime, effects of external mass transfer, heat removal and pressure drop and sphere catalyst arrangement in reactor in macro scale.

References

[1] IMechE, Climate change adapting to the inevitable? . Institution of Mechanical Engineering, 2013: p. 30.

[2] E.I.A, International Energy Outlook with projection to 2040. United States Energy Information Administration, 2013: p. 312.

[3] N. Moazami, et al., Mathematical Modeling and Performance Study of Fischer-tropsch Synthesis of Liquid Fuel over Cobalt-silica. Energy Procedia, 2015. 75: p. 62-71.

[4] S. Czernik and A. Bridgwater, Overview of applications of biomass fast pyrolysis oil. Energy & Fuels, 2004. 18(2): p. 590-598.

[5] O. Doustdar, M.L. Wyszynski, H. Mahmoudi, and A. Tsolakis, Enhancing the properties of Fischer-Tropsch fuel produced from syngas over Co/SiO2 catalyst: Lubricity and Calorific Value, in IOP Conference Series: Materials Science and Engineering. 2016. p. 012092.

[6] Hessam Jahangiri, James Bennett, Parvin Mahjoubi, Karen Wilson, and S. Gu, A review of advanced catalyst development for Fischer–Tropsch synthesis of hydrocarbons from biomass derived syn-gas. The Royal Society of Chemistry, 2014.

[7] N. Moazami, et al., Modelling of a fixed bed reactor for Fischer–Tropsch synthesis of simulated N2-rich syngas over Co/SiO2: Hydrocarbon production. Fuel, 2015. 154: p. 140-151.

[8] A.N. Stranges, A history of the fischer-tropsch synthesis in Germany 1926-45. Studies in surface science and catalysis, 2007: p. 1-27.

[9] H. Mahmoudi, Perfomance of cobalt-based eggshell catalyst in low temperature Fischer tropsch synthesis process to produce long-chain hydrocarbons from synthesis gas utilizing fixed-bed reactor technology, in School of Mechanical Engineering. 2015, The University of Birmingham.

[10] J. Perritano. Top 10 Advantages of Biofuels. [cited 2014; Available from: http://www.howstuffworks.com/.

[11] A. Murugesan, C. Umarani, R. Subramanian, and N. Nedunchezhian, Bio-diesel as an alternative fuel for diesel engines—A review. Renewable and Sustainable Energy Reviews, 2009. 13(3): p. 653-662.

[12] S. Gill, A. Tsolakis, K. Dearn, and J. Rodríguez-Fernández, Combustion characteristics and emissions of Fischer–Tropsch diesel fuels in IC engines. Progress in Energy and Combustion Science, 2011. 37(4): p. 503-523.

[13] M. Lapuerta, O. Armas, J.J. Hernández, and A. Tsolakis, Potential for reducing emissions in a diesel engine by fuelling with conventional biodiesel and Fischer–Tropsch diesel. Fuel, 2010. 89(10): p. 3106-3113.

[14] Y.H. Kim, K.-W. Jun, H. Joo, C. Han, and I.K. Song, A simulation study on gas-to-liquid (natural gas to Fischer–Tropsch synthetic fuel) process optimization. Chemical Engineering Journal, 2009. 155(1): p. 427-432.

[15] X. Li, Z. Huang, J. Wang, and W. Zhang, Particle size distribution from a GTL engine. Science of the total environment, 2007. 382(2): p. 295-303.

[16] DECC. Reducing the UK's greenhouse gas emissions by 80% by 2050. 2014 [cited 2014 20 May]; Available from: www.gov.uk

[17] JNCC, The global biodiversity footprint of UK biofuel consumption. Joint Nature Conservation Committee, 2009: p. 40.

[18] J. Runyon. 2011 Outlook for Clean Energy Jobs in the U.S. – Beating the Trend. 2010 November 12 [cited 2014 20 May]; Available from: www. renewableenergyworld.com

[19] P. Basu, Biomass gasification and pyrolysis: practical design and theory. 2010: Academic press.

[20] DECC, Use of UK biomass for electricity and CHP. Department of Energy and Climate Change, 2013: p. 9.

[21] M.H. Rafiq, H.A. Jakobsen, R. Schmid, and J.E. Hustad, Experimental studies and modeling of a fixed bed reactor for Fischer–Tropsch synthesis using biosyngas. Fuel processing technology, 2011. 92(5): p. 893-907.

[22] G.P. van der Laan, Kinetics, selectivity and scale up of the Fischer-Tropsch synthesis. 1999: [University Library Groningen][Host].

[23] X. Wang and M. Economides, Advanced Natural Gas Engineering. 2013: Elsevier.

[24] B.H. Davis, Fischer–Tropsch synthesis: current mechanism and futuristic needs. Fuel Processing Technology, 2001. 71(1): p. 157-166.

[25] H. Taylor, Catalysis. Volume IV. Hydrocarbon Synthesis, Hydrogenation and Cyclization. Journal of the American Chemical Society, 1957. 79(3): p. 760-760.

[26] A. de Klerk, Fischer-Tropsch Refining. 2012: John Wiley & Sons.

[27] R.B. Anderson, H. Kölbel, and M. Ralek, The Fischer-Tropsch Synthesis. Vol. 16. 1984: Academic Press New York.

[28] G.H. Olivé and S. Olive, The chemistry of the catalyzed hydrogenation of carbon monoxide. Springer, Berlin, 1984. 143: p. 176.

[29] J. Yang, W. Ma, D. Chen, A. Holmen, and B.H. Davis, Fischer–Tropsch synthesis: A review of the effect of CO conversion on methane selectivity. Applied Catalysis A: General, 2014. 470: p. 250-260.

[30] A. Raje, J.R. Inga, and B.H. Davis, Fischer-Tropsch synthesis: process considerations based on performance of iron-based catalysts. Fuel, 1997. 76(3): p. 273-280.

[31] N. Moazami, et al., Catalytic performance of cobalt–silica catalyst for Fischer–Tropsch synthesis: Effects of reaction rates on efficiency of liquid synthesis. Chemical Engineering Science, 2015. 134: p. 374-384.

[32] S. Storsæter, D. Chen, and A. Holmen, Microkinetic modelling of the formation of C< sub> 1</sub> and C< sub> 2</sub> prod-

ucts in the Fischer–Tropsch synthesis over cobalt catalysts. Surface science, 2006. 600(10): p. 2051-2063.
[33] M. Kollár, et al., The mechanism of the Fischer–Tropsch reaction over supported cobalt catalysts. Journal of Molecular Catalysis A: Chemical, 2010. 333(1): p. 37-45.
[34] J. Yang, et al., Reaction mechanism of CO activation and methane formation on Co Fischer–Tropsch catalyst: a combined DFT, transient, and steady-state kinetic modeling. Journal of Catalysis, 2013. 308: p. 37-49.
[35] C.K. Rofer-DePoorter, A comprehensive mechanism for the Fischer-Tropsch synthesis. Chemical Reviews, 1981. 81(5): p. 447-474.
[36] E.F. Vansant, P. Van Der Voort, and K.C. Vrancken, Characterization and chemical modification of the silica surface. 1995: Elsevier.
[37] L. Zhuravlev, The surface chemistry of amorphous silica. Zhuravlev model. Colloids and Surfaces A: Physicochemical and Engineering Aspects, 2000. 173(1): p. 1-38.
[38] D. Michel, V. Kazansky, and V. Andreev, Study of the interaction between surface hydroxyls and adsorbed water molecules on porous glasses by means of infrared spectroscopy. Surface Science, 1978. 72(2): p. 342-356.
[39] N. Sheppard, Some studies of physical and chemical adsorption by means of infra-red spectroscopy. Chimie Pure Et Appliquée, 1962. 4: p. 71.
[40] V.Y. Davydov, A. Kiselev, and L. Zhuravlev, Study of the surface and bulk hydroxyl groups of silica by infra-red spectra and D2O-exchange. Transactions of the Faraday Society, 1964. 60: p. 2254-2264.
[41] H.E. Bergna, The Colloid Chemistry of Silica. Advances in Chemistry Series 234, ed. M.J. Comstock. Vol. 234. 1994, Washington, DC: American Chemical Society. 669.
[42] J. Peri and A. Hensley Jr, The surface structure of silica gel. The Journal of Physical Chemistry, 1968. 72(8): p. 2926-2933.
[43] B. Morrow and A. McFarlan, Chemical reactions at silica surfaces. Journal of non-crystalline solids, 1990. 120(1): p. 61-71.
[44] L. Zhuravlev, Structurally bound water and surface characterization of amorphous silica. Pure Appl Chem, 1989. 61: p. 1969-1976.
[45] J. Nawrocki, The silanol group and its role in liquid chromatography. Journal of Chromatography A, 1997. 779(1): p. 29-71.
[46] K. Unger, K. Lork, B. Pfleiderer, K. Albert, and E. Bayer, Impact of acidic/hydrothermal treatment on pore structural and chromatographic properties of porous silicas: I. The conventional approach. Journal of Chromatography A, 1991. 556(1): p. 395-406.
[47] V.M. Bermudez, Proton nuclear magnetic resonance technique for determining the surface hydroxyl content of hydrated silica gel. The Journal of Physical Chemistry, 1970. 74(23): p. 4160-4161.
[48] M.L. Hair, Hydroxyl groups on silica surface. Journal of Non-Crystalline Solids, 1975. 19: p. 299-309.
[49] P. Der Voort, Modelling of the hydroxyl group population using an energetic analysis of the temperature-programmed desorption of pyridine from silica gel. Journal of the Chemical Society, Faraday Transactions, 1992. 88(5): p. 723-727.
[50] I.-S. Chuang and G.E. Maciel, A detailed model of local structure and silanol hydrogen bonding of silica gel surfaces. The Journal of Physical Chemistry B, 1997. 101(16): p. 3052-3064.
[51] M.E. Dry, Catalytic aspects of industrial Fischer-Tropsch synthesis. Journal of Molecular Catalysis, 1982. 17(2–3): p. 133-144.
[52] E. van Steen and M. Claeys, Fischer-Tropsch Catalysts for the Biomass-to-Liquid (BTL)-Process. Chemical engineering & technology, 2008. 31(5): p. 655-666.
[53] R. Guettel, U. Kunz, and T. Turek, Reactors for Fischer-Tropsch Synthesis. Chemical Engineering & Technology, 2008. 31(5): p. 746-754.
[54] C. Perego, R. Bortolo, and R. Zennaro, Gas to liquids technologies for natural gas reserves valorization: The Eni experience. Catalysis Today, 2009. 142(1): p. 9-16.
[55] W.C. Content, Petroleum Technology, vol. 2. 2007, Wiley & Sons, Hoboken, NJ.
[56] A.Y. Khodakov, A. Griboval-Constant, R. Bechara, and V.L. Zholobenko, Pore size effects in Fischer Tropsch synthesis over cobalt-supported mesoporous silicas. Journal of Catalysis, 2002. 206(2): p. 230-241.
[57] Y.-N. Wang, Y.-Y. Xu, H.-W. Xiang, Y.-W. Li, and B.-J. Zhang, Modeling of catalyst pellets for Fischer-Tropsch synthesis. Industrial & engineering chemistry research, 2001. 40(20): p. 4324-4335.
[58] Z. Qu, et al., Enhancement of the catalytic performance of supported-metal catalysts by pretreatment of the support. Journal of Catalysis, 2005. 234(1): p. 33-36.
[59] A. Saib, M. Claeys, and E. Van Steen, Silica supported cobalt Fischer–Tropsch catalysts: effect of pore diameter of support. Catalysis today, 2002. 71(3): p. 395-402.
[60] B.C. Dunn, et al., Silica aerogel supported catalysts for Fischer–Tropsch synthesis. Applied Catalysis A: General, 2005. 278(2): p. 233-238.
[61] E. Peluso, C. Galarraga, and H. De Lasa, Eggshell catalyst in Fischer–Tropsch synthesis: Intrinsic reaction kinetics. Chemical engineering science, 2001. 56(4): p. 1239-1245.
[62] K. Triantafyllidis, A. Lappas, and M. Stöcker, The Role of Catalysis for the Sustainable Production of Bio-fuels and Biochemicals. 2013: Newnes.
[63] S.A. Gardezi, J.T. Wolan, and B. Joseph, Effect of catalyst preparation conditions on the performance of eggshell cobalt/SiO< sub> 2</sub> catalysts for Fischer–Tropsch synthesis. Applied Catalysis A: General, 2012. 447: p. 151-163.
[64] D. Song and J. Li, Effect of catalyst pore size on the catalytic performance of silica supported cobalt Fischer–Tropsch catalysts. Journal of Molecular Catalysis A: Chemical, 2006. 247(1): p. 206-212.
[65] J.-S. Girardon, et al., Effect of cobalt precursor and pretreatment conditions on the structure and catalytic performance of cobalt silica-supported Fischer–Tropsch catalysts. Journal of Catalysis, 2005. 230(2): p. 339-352.
[66] Y. Zhang, Y. Liu, G. Yang, S. Sun, and N. Tsubaki, Effects of impregnation solvent on Co/SiO2 catalyst for Fischer-Tropsch synthesis: A highly active and stable catalyst with bimodal sized cobalt particles. Applied Catalysis A: General, 2007. 321(1): p. 79-85.
[67] J.-S. Jung, S.W. Kim, and D.J. Moon, Fischer–Tropsch Synthesis over cobalt based catalyst supported on different mesoporous silica. Catalysis Today, 2012. 185(1): p. 168-174.
[68] A.M. Venezia, et al., Co/SiO2 catalysts for Fischer–Tropsch synthesis; effect of Co loading and support modification by TiO2. Catalysis Today, 2012. 197(1): p. 18-23.
[69] S. Sun, N. Tsubaki, and K. Fujimoto, The reaction performances and characterization of Fischer–Tropsch synthesis Co/SiO2 cat-

alysts prepared from mixed cobalt salts. Applied Catalysis A: General, 2000. 202(1): p. 121-131.
[70] Y. Zhang, Y. Liu, G. Yang, Y. Endo, and N. Tsubaki, The solvent effects during preparation of Fischer–Tropsch synthesis catalysts: Improvement of reducibility, dispersion of supported cobalt and stability of catalyst. Catalysis Today, 2009. 142(1): p. 85-89.
[71] H. Ming, B.G. Baker, and M. Jasieniak, Characterization of cobalt Fischer–Tropsch catalysts: 2. Rare earth-promoted cobalt-silica gel catalysts prepared by wet impregnation. Applied Catalysis A: General, 2010. 381(1): p. 216-225.
[72] A. Jess and C. Kern, Modeling of Multi-Tubular Reactors for Fischer-Tropsch Synthesis. Chemical engineering & technology, 2009. 32(8): p. 1164-1175.
[73] J.H. Yang, et al., Mass transfer limitations on fixed-bed reactor for Fischer–Tropsch synthesis. Fuel Processing Technology, 2010. 91(3): p. 285-289.
[74] S. Chambrey, et al., Fischer–Tropsch synthesis in milli-fixed bed reactor: Comparison with centimetric fixed bed and slurry stirred tank reactors. Catalysis Today, 2011. 171(1): p. 201-206.
[75] A. Jess, R. Popp, and K. Hedden, Fischer–Tropsch-synthesis with nitrogen-rich syngas: fundamentals and reactor design aspects. Applied Catalysis A: General, 1999. 186(1): p. 321-342.
[76] C.N. Satterfield, G.A. Huff Jr, H.G. Stenger, J.L. Carter, and R.J. Madon, A comparison of Fischer-Tropsch synthesis in a fixed-bed reactor and in a slurry reactor. Industrial & engineering chemistry fundamentals, 1985. 24(4): p. 450-454.
[77] O. González, et al., Use of different mesostructured materials based on silica as cobalt supports for the Fischer–Tropsch synthesis. Catalysis Today, 2009. 148(1–2): p. 140-147.
[78] N. Osakoo, R. Henkel, S. Loiha, F. Roessner, and J. Wittayakun, Palladium-promoted cobalt catalysts supported on silica prepared by impregnation and reverse micelle for Fischer–Tropsch synthesis. Applied Catalysis A: General, 2013. 464–465(0): p. 269-280.
[79] H. Wu, et al., Effect of TiO2 promotion on the structure and performance of silica-supported cobalt-based catalysts for Fischer–Tropsch synthesis. Journal of Molecular Catalysis A: Chemical, 2014. 390(0): p. 52-62.
[80] A.Y. Khodakov, R. Bechara, and A. Griboval-Constant, Fischer–Tropsch synthesis over silica supported cobalt catalysts: mesoporous structure versus cobalt surface density. Applied Catalysis A: General, 2003. 254(2): p. 273-288.
[81] W. Ma, et al., Fischer–Tropsch synthesis: Support and cobalt cluster size effects on kinetics over Co/Al2O3 and Co/SiO_2 catalysts. Fuel, 2011. 90(2): p. 756-765.
[82] J. Hong, et al., Impact of sorbitol addition on the structure and performance of silica-supported cobalt catalysts for Fischer–Tropsch synthesis. Catalysis Today, 2011. 175(1): p. 528-533.
[83] M.K. Gnanamani, G. Jacobs, W.D. Shafer, and B.H. Davis, Fischer–Tropsch synthesis: Activity of metallic phases of cobalt supported on silica. Catalysis Today, 2013. 215(0): p. 13-17.
[84] J. van de Loosdrecht, et al., Cobalt Fischer-Tropsch synthesis: Deactivation by oxidation? Catalysis Today, 2007. 123(1–4): p. 293-302.
[85] S. Storsæter, B. Tøtdal, J.C. Walmsley, B.S. Tanem, and A. Holmen, Characterization of alumina-, silica-, and titania-supported cobalt Fischer–Tropsch catalysts. Journal of Catalysis, 2005. 236(1): p. 139-152.
[86] P. Hunpinyo, et al., A comprehensive small and pilot fixed bed reactor approach for testing Fischer-Tropsch catalyst activity and performance on BTL route. Arabian Journal of Chemistry, (0).
[87] N.O. Elbashir, B. Bao, and M.M. El-Halwagi, An Approach to the Design of Advanced Fischer-Tropsch Reactor for Operation in Near-Critical and Supercritical Phase Media, in Proceedings of the 1st Annual Gas Processing Symposium, H.E. Alfadala, G.V.R. Reklaitis, and M.M. El-Halwagi, Editors. 2009, Elsevier: Amsterdam. p. 423-433.
[88] R. Guettel and T. Turek, Comparison of different reactor types for low temperature Fischer–Tropsch synthesis: A simulation study. Chemical Engineering Science, 2009. 64(5): p. 955-964.
[89] H. Schulz, Short history and present trends of Fischer–Tropsch synthesis. Applied Catalysis A: General, 1999. 186(1–2): p. 3-12.
[90] W. Chu, et al., Cobalt species in promoted cobalt alumina-supported Fischer–Tropsch catalysts. Journal of Catalysis, 2007. 252(2): p. 215-230.
[91] Y. Zhang, H. Xiong, K. Liew, and J. Li, Effect of magnesia on alumina-supported cobalt Fischer–Tropsch synthesis catalysts. Journal of Molecular Catalysis A: Chemical, 2005. 237(1–2): p. 172-181.
[92] S.S. Itkulovaa, G.D. Zakumbaevaa, R.S. Arzumanovab, and V.A. Ovchinnikovb, Production of hard hydrocarbons from synthesis-gas over co-containing supported catalysts. Fischer-Tropsch Synthesis, Catalysts and Catalysis, 2006. 163: p. 75.
[93] H. Schulz, Comparing Fischer-Tropsch synthesis on iron-and cobalt catalysts: The dynamics of structure and function. Studies in surface science and catalysis, 2007. 163: p. 177-199.
[94] G. Jacobs, et al., Fischer-Tropsch synthesis: influence of support on the impact of co-fed water for cobalt-based catalysts. Fischer-Tropsch Synthesis, Catalysts and Catalysis, 2006. 163: p. 217.